IEEE Access
Multidisciplinary | Rapid Review | Open Access Journal

Received September 1, 2018, accepted September 23, 2018, date of publication October 5, 2018, date of current version November 9, 2018.

Digital Object Identifier 10.1109/ACCESS.2018.2873660

Decentralized Adaptive Quantized Excitation Control for Multi-Machine Power Systems by Considering the Line-Transmission Delays

XIUYU ZHANG[1], (Member, IEEE), BIN LI[1], GUOQIANG ZHU[1], XINKAI CHEN[2], (Senior Member, IEEE), AND MIAOLEI ZHOU[3], (Member, IEEE)

[1]School of Automation Engineering, Northeast Electric Power University, Jilin 132012, China
[2]Department of Electronic and Information Systems, Shibaura Institute of Technology, Saitama 337-8570, Japan
[3]Department of Control Science and Engineering, Jilin University, Changchun 130012, China

Corresponding authors: Guoqiang Zhu (zhugqcn@gmail.com) and Xinkai Chen (chen@shibaura-it.ac.jp)

This work was supported in part by the National Natural Science Foundation of China under Grant 61673101, in part by the Science and Technology Project of Jilin Province under Grant 20180201009SF, Grant 20170414011GH, and Grant 20180201004SF, in part by the Thirteenth Five Year Science Research Plan of Jilin Province under Grant JJKH20170105KJ, in part by the Jilin Technological Innovation Development Plan under Grant 201831719, and in part by the JSPS under Grant C-15K06152 and Grant 14032011-000073.

ABSTRACT In this paper, a neural decentralized adaptive quantized dynamic surface control scheme is proposed for a class of large-scale multi-machine power systems with static var compensator (SVC) and unknown line-transmission time delays. The main contributions of the proposed method are summarized as follows: 1) a decentralized dynamic surface quantized control scheme with simple structure is proposed for the large-scale multi-machine systems with SVC, where the ''explosion of complexity'' problem in backstepping method and the complexities introduced by SVC are overcome; 2) the unknown line-transmission time delays between different generators are considered and dealt with by introducing the finite-cover lemma with radial basis function neural networks (RBFNNs) approximator, which leads to the arbitrarily small $\mathcal{L}_\infty$[a] tracking performance; 3) the strong nonlinearities, uncertain parameters and external disturbances of the system are considered and the number of the estimated parameters is greatly reduced by estimating the weight vector norm of neural networks instead of estimating the weighted vector itself. It is proved that all the signals in the control system are ultimately uniformly bounded[b] and can be made arbitrarily small. Simulation results show the validity of the proposed method.

INDEX TERMS Dynamic surface control (DSC), large-scale multi-machine power system, $\mathcal{L}_\infty$ tracking performance, static var compensator (SVC), hysteresis quantizer.

I. INTRODUCTION

With the rapid expansion of the scales of power grid, the control of large-scale multi-machine power systems has attracted much attention due to the properties of the strong nonlinearities and multiple coupled characteristics in the large-scale power systems [1]–[6]. Generally, centralized and decentralized control methods are the main tools to cope with the above control problems because the equipments of power systems are distributed in different areas. In the centralized control for large-scale power systems, poor knowledge of different generator parameters and interactions from different subsystems are the difficulties to cope with. For example, if each subsystem is distributed distantly, it is difficult for a centralized controller to gather exact feedback signals from all the subsystems timely. Also the design and implementation of the centralized controller are complicated as pointed out by [7]. Therefore, decentralized control become a popular method in the controller design for large-scale multi-machine power systems. Some related results have been achieved for the power systems such as in [8], a Lyapunov-based decentralized excitation controller is developed for the

[a]Here, the $\mathcal{L}_\infty$ norm is defined as $\|x\|_\infty \triangleq \sup_{t\geq 0}|x(t)|$ and we say $x \in \mathcal{L}_\infty$ when $\|x\|_\infty$ exists.

[b]Here, we say $x(t)$ is ultimately uniformly bounded if there exist positive constants b and c, independent of $t_0 \geq 0$, and for every $a \in (0, c)$, there is $T = T(a, b)$, independent of t_0, such that $\|x(t_0)\| \leq a \Rightarrow \|x(t)\| \leq b$, $\forall t \geq t_0 + T$.

multi-machine power systems where only the local measurements were considered. On the other hand, the uncertainties and the unmeasurable parameters of the power systems leads to the combination of the adaptive control [9], [10] and decentralized control for the power systems since the first decentralized adaptive control scheme was proposed in [11]. In [12], a radial basis function neural networks (RBFNNs) based decentralized adaptive dynamic surface control scheme is proposed for the multi-machine power system. In [13], to achieve decentralization, each generator is modeled as an independent uncertain dynamic subsystem, where the uncertainty is treated as a disturbance and this disturbance represents the effect from other subsystems. However, the time delays on the line-transmission are not considered.

It is well known that time delays are common physical phenomena and widely exist in many practical systems such as the large-scale multi-machine power systems (time delays may be as high as dozens or even hundreds of milliseconds). The existence of time delays may degrade the control accuracy and even leads to instability of control systems. Therefore, it is a challenging work to mitigate the influence of time delays in large-scale multi-machine power systems. Generally, the most common method to deal with time delays is the Krasovskii functionals and Razumikhin functionals such as [14]–[16]. However, the arbitrarily small tracking performance for all $t > 0$ was failed to obtain.

Also, the SVC plays an important role in maintaining the stability of voltages in the power systems [17], [18] and improving the transient stability [19]–[21]. When the SVC is equipped in the power systems, the electrical power quality can be improved. However, the uncertainties and complexities of the power systems are enhanced. In addition, the computer control become more and more important with the development of Network and information technology. Hence, in order to realize the computer control for large-scale multi-machine power systems with SVC the control signals are required quantized before they go through communication channels [7], [22]–[26]. A quantizer maps a continuous signal to a discrete finite set where a piecewise constant function of time is included. As a new transformed input of the control systems, the quantizer generates strong nonlinearities and leads to poor tracking performance or even instability [27]. To our best knowledge, no related results are available for decentralized adaptive quantized controller design for the large-scale multi-machine power systems with SVC when the transmission time delays are considered.

To address the above control problems, in this paper, a decentralized adaptive quantized control dynamic surface control scheme, which is a recursive and step by step design procedure with respect to the orders of the control systems [28], [29], is proposed for the large-scale power systems with SVC and the transmission time delays. The main contributions are summarized as follows:

- By constructing the modified hysteresis quantizer and introducing the first-order low pass filters as [28] and [29], a computer-control based decentralized adaptive dynamic surface control scheme for the large scale power systems with SVC is firstly proposed, where the ''explosion of complexity'' problem in backstepping methods, the uncertainties and complexities introduced by SVC are overcome. Also, the structure of the controller is simplified due to the use of the first-order low pass filter.
- The time delays on the transmission lines is considered and by combining the finite-cover lemma with the radial basis function neural networks (RBFNNs) approximator, the traditional Krasovskii functionals and Razumikhin functions are abandoned when dealing with the unknown time delays. Then, the unknown time delay functions are estimated on-line and the arbitrarily small $\mathcal{L}_\infty$ tracking performance is achieved by introducing the initialization technique.
- By estimating the weight vector norm of neural networks instead of the weight vector itself, the number of the estimated parameters is greatly reduced, leading to the reduction of the computational burden.

The remainder of this paper is organized as follows. In Section 2, the RBFNNs, the hysteresis quantizer, the mathematical preliminaries and the mathematical model of large-scale multi-machine systems considering the SVC and transmission time delays are described. In Section 3, the decentralized adaptive quantized controller design procedures are presented by employing the dynamic surface control method. Section 4 shows the analysis of stability. Section 5 illustrates the simulation results to demonstrate the effectiveness of the proposed scheme. The conclusion is formulated in Section 6.

II. PROBLEM STATEMENT AND PRELIMINARIES

A. MATHEMATICAL MODELS

As shown in [30], the model of large-scale power systems with SVC is described by the following differential equations:

$$\begin{aligned}
\dot{\delta}_i(t) &= \omega_i - \omega_0, \\
\dot{\omega}_i(t) &= \frac{\omega_0}{2H_i}(P_{mi} - P_{ei}) - \frac{D_i}{2H_i}\omega_i(t) + d_i, \\
\dot{E}'_{qi}(t) &= \frac{1}{T'_{doi}}\left[E_{fi}(t) - E_{qi}(t)\right],
\end{aligned} \tag{1}$$

where d_i denotes the external disturbance. Considering the transmission delays between different generators, the electrical equations are described as:

$$\begin{aligned}
E_{fi}(t) &= k_{ei}u_{fi}(t), \\
I_{qi}(t) &= \sum_{j=1}^{n} E'_{qi}(t) B_{ij} \sin\left(\delta_i - \delta_j\left(t - \tau_{j/i}\right)\right), \\
E_{qi}(t) &= E'_{qi}(t) + \left(x_{di} - x'_{di}\right) I_{di}(t) = x_{adi} I_{fi}(t),
\end{aligned}$$

TABLE 1. The notation for large-scale multi-machine power systems.

Nomenclature	
δ_i	the power angle, in rad
ω_i	the relative speed of the generator, in rad/s
$\omega_0 = 2\pi f_0$	the synchronous machine speed, in rad/s
f_0	the rated frequency (Hz)
D_i	the per unit damping constant
H_i	the inertia constant, in s
P_{mi}	the mechanical input power, in p.u. (per unit)
P_{ei}	the electrical power, in p.u.
E'_{qi}	the q-axis internal transient electric potential, in p.u.
E_{qi}	the EMF in the quadrature axis, in p.u.
E_{fi}	the equivalent EMF in the excitation coil, in p.u.
x_{adi}	the mutual reactance between the excitation coil and the stator coil, in p.u.
T'_{doi}	the direct axis transient short-circuit time constant, in s
Q_{ei}	the reactive power, in p.u.
I_{qi}	the quadrature axis current, in p.u.
I_{di}	the direct axis current, in p.u.
B_{ij}	the ith row and jth column element of nodal suseptancen matrix at the internal nodes after eliminating all physical buses, in p.u.
B_{Li}	the adjustable equivalent susceptance in SVC
B_{Ci}	the initial value of adjustable susceptance
u_{fi}	the input of the SCR amplifier, in p.u.
u_{Bi}	the input of SVC, in p.u.
x_{di}	the direct axis reactance, in p.u.
x'_{di}	the direct axis transient reactance, in p.u.

$$
\begin{aligned}
I_{di}(t) &= -\sum_{j=1}^{n} E'_{qj}(t) B_{ij} \cos\left(\delta_i - \delta_j\left(t-\tau_{j/i}\right)\right),\\
P_{ei}(t) &= \sum_{j=1}^{n} E'_{qi}(t) E'_{qj}\left(t-\tau_{j/i}\right) B_{ij} \sin\left(\delta_i - \delta_j\left(t-\tau_{j/i}\right)\right),\\
Q_{ei}(t) &= -\sum_{j=1}^{n} E'_{qi}(t) E'_{qj}\left(t-\tau_{j/i}\right) B_{ij} \cos(\delta_i - \delta_j\left(t-\tau_{j/i}\right))
\end{aligned}
\tag{2}
$$

and the SVC models are shown as follows [31]:

$$
\dot{B}_{Li} = \frac{1}{T_{\mathrm{Ci}}}\left(-B_{Li} + B_{\mathrm{Ci}} + u_{Bi}\right), \tag{3}
$$

where $i = 1, 2, \cdots, n$ with n denoting the number of interconnected generators, $\tau_{j/i}$, $i, j = 1, 2, \cdots, n$, denoting the transmission delays from the jth generator to the ith generator. The notation for large-scale multi-machine power systems in (1)-(3) is given in Table 1.

B. MODEL FOR EXCITATION CONTROLLER DESIGN AND LEMMA

Let $\Delta P_{ei} = P_{ei} - P_{mi0}$ with $P_{mi0} = P_{mi}$ to be a constant. Then, it follows that [30]–[32]

$$
\begin{aligned}
\dot{\delta}_i(t) &= \omega_i - \omega_0,\\
\dot{\omega}_i &= -\frac{D_i}{2H_i}\omega_i - \frac{\omega_0}{2H_i}\Delta P_{ei} + d_i,\\
\Delta\dot{P}_{ei}(t) &= -\frac{1}{T'_{doi}}\Delta P_{ei}(t) + \frac{1}{T'_{doi}}u_i\\
&\quad + h_i\left(\delta_i(t), \delta_j\left(t-\tau_{j/i}\right), \omega_j\left(t-\tau_{j/i}\right)\right),
\end{aligned}
\tag{4}
$$

where u_i is the control signal with

$$
u_i = I_{qi}E_{fi} - \left(x_{di} - x'_{di}\right) I_{di} I_{qi} - P_{mi} - T'_{doi} Q_{ei}\omega_i, \tag{5}
$$

and

$$
\begin{aligned}
&h_i\left(\delta_i(t), \delta_j\left(t-\tau_{j/i}\right), \omega_j\left(t-\tau_{j/i}\right)\right)\\
&= E'_{qi}\sum_{j=1}^{n}\dot{E}'_{qj}(t) B_{ij}\sin(\delta_i(t) - \delta_j\left(t-\tau_{j/i}\right))\\
&\quad - E'_{qi}\sum_{j=1}^{n} E'_{qj}(t) B_{ij}\cos(\delta_i(t) - \delta_j\left(t-\tau_{j/i}\right))\omega_j\left(t-\tau_{j/i}\right).
\end{aligned}
\tag{6}
$$

being the interconnected terms which satisfies [30]–[32]

$$
\begin{aligned}
&\left|h_i\left(\delta_i(t), \delta_j\left(t-\tau_{j/i}\right), \omega_j\left(t-\tau_{j/i}\right)\right)\right|\\
&\le \sum_{j=1, j\neq i}^{n}\frac{4}{\left|T'_{doj}\right|_{\min}}|P_{ei}|_{\max}\left|\sin(\delta_i(t) - \delta_j\left(t-\tau_{j/i}\right))\right|\\
&\quad + \sum_{j=1}^{n}|Q_{ei}|_{\max}\left|\omega_j\left(t-\tau_{j/i}\right)\right|\\
&\le \sum_{j=1}^{n}\frac{4p_{1ij}}{\left|T'_{doj}\right|_{\min}}|P_{ei}|_{\max}\left(|\sin(\delta_i(t))| + \left|\delta_j\left(t-\tau_{j/i}\right)\right|\right)\\
&\quad + \sum_{j=1}^{n}p_{2ij}|Q_{ei}|_{\max}\left|\omega_j\left(t-\tau_{j/i}\right)\right|\\
&= \sum_{j=1}^{n}(\gamma_{i1j}(\left|\delta_j\left(t-\tau_{j/i}\right)\right|) + \gamma_{i2}\left|\omega_j\left(t-\tau_{j/i}\right)\right|).
\end{aligned}
\tag{7}
$$

Therein,

$$
\begin{aligned}
\gamma_{i1j} &= \begin{cases}\displaystyle\sum_{j=1, j\neq i}^{n}\frac{4p_{1ij}}{\left|T'_{doj}\right|_{\min}}|P_{ei}|_{\max}, & \text{when } j = i,\\ \dfrac{4p_{1ij}}{\left|T'_{doj}\right|_{\min}}|P_{ei}|_{\max}, & \text{when } j \neq i,\end{cases}\\
\gamma_{i2} &= p_{2ij}|Q_{ei}|_{\max}
\end{aligned}
\tag{8}
$$

and p_{1ij}, p_{2ij} are constants with values either 1 or 0.

Let $x_{i1} = \delta_i - \delta_{i0}$, $x_{i2} = \omega_i - \omega_0$, $x_{i3} = P_{ei} - P_{mio}$, $x_{i4} = V_{mi} - V_{refi}$,

$$
V_{mi} = \frac{\sqrt{\left(X_{2i}E'_{qi}\right)^2 + (X_{1i})^2 + 2X_{1i}X_{2i}E'_{qi}\cos x_{i1}}}{X'_{d\Sigma}}, \tag{9}
$$

where V_{mi} and V_{refi} are the accessing point voltage and the corresponding reference voltage of the SVC, respective; $X_{1i} = x'_{di} + X_{Ti}$, $X'_{d\Sigma i} = X_{1i} + X_{2i} + X_{1i}X_{2i}\left(B_{Li} - B_{\mathrm{Ci}}\right)$ with X_{2i} being the transmission line reactance and X_{Ti} being the transformer reactance.

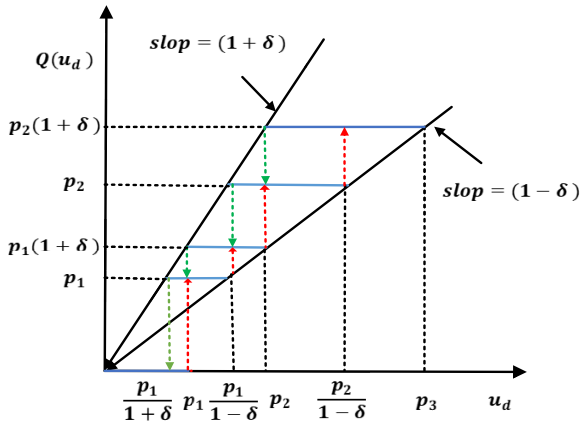

FIGURE 1. Hysteresis quantizer.

C. HYSTERESIS QUANTIZER DESCRIPTION

In this paper, the hysteresis quantizer is employed and described as follows [33], [34].

$$Q_i(u_i) = \begin{cases} p_{i,j}, & \text{if } \dfrac{p_{i,j}}{1+\delta_i} < u_i \le p_{i,j}, \\ & Q_i^- \ge p_{i,j} \text{ or } Q_i^- \le p_{i,j} \\ & p_{i,j} \le u_i < \dfrac{p_{i,j}}{1-\delta_i}, \\ (1+\sigma_i)\, p_{i,j}, & \text{if } p_{i,j} < u_i \le \dfrac{p_{i,j}}{1-\delta_i}, \\ & Q_i^- \ge (1+\sigma_i)\, p_{i,j}, \\ & \text{or } \dfrac{p_{i,j}}{1-\delta_i} \le u_i < p_{i,j+1}, \\ & Q_i^- \le (1+\sigma_i)\, p_{i,j}, \\ 0, & \text{if } 0 \le u_i \le \dfrac{p_{i,1}}{1+\delta_i} \\ & \text{or } \dfrac{p_{i,1}}{1+\delta_i} < u_i < p_{i,1}, \\ & Q_i^- = 0, \\ -Q_i(-u_i), & \text{if } u_i < 0, \end{cases} \tag{10}$$

where $\delta_i = \frac{1-\epsilon_i}{1+\epsilon_i}$ and $p_{i,j} = a_i \epsilon_i^{1-j}$, $j = 1, 2, 3 \cdots$ with $0 < \epsilon_i < 1$, $a_i > 0$. The parameter a_i determines the size of the dead-zone for $Q_i(u_i)$, and ϵ_i is a measure of quantization density.The smaller the ϵ_i is, the coarser the quantizer is. In (10), $Q_i^-(t)$ is the latest value of Q_i before the time instant t and $Q_i^-(0) := 0$. Mathematically, $Q_i^-(t) = 0$ for $t \in [0, T_{i,1}]$ and $Q_i^-(t) = Q_i(u_i(T_{i,h}))$ for $t \in (T_{i,h}, T_{i,h+1}]$, where $T_{i,h}$ $(h = 1, 2, 3, \cdots)$ with $0 \le T_{i,1} < T_{i,2} < T_{i,3} < \cdots \le +\infty$ denote the time instants when $Q_i(u_i)$ make transitions. The maps of (10) for $u_i \ge 0$ are plotted in FIGURE 1.

Here, let the maximum values of $a_i(t)$ and $\epsilon_i(t)$ be $\bar{a}_i$ and $\bar{\epsilon}_i$ and the minimum values be $\underline{a}_i$ and $\underline{\epsilon}_i$. Then, we have

$$0 < \underline{a}_i \le a_i(t) \le \bar{a}_i, \quad 0 < \underline{\epsilon}_i \le \epsilon_i(t) \le \bar{\epsilon}_i < 1, \ \forall t \ge 0. \tag{11}$$

We emphasize that different with the logarithmic quantizer in [37], the hysteresis quantizer (10) in this paper has additional quantization levels and can reduce chattering because whenever the output of the quantizer takes a transition between two different values, some dwelling time will elapse before a new transition occurs.

As shown in [30]–[32] by using (5)-(9), and the hysteresis quantizer in (10), (4) can be rewritten as

$$\begin{aligned} \dot{x}_{i1} &= x_{i2}, \\ \dot{x}_{i2} &= f_{i2}(\bar{x}_{i2}) - g_{i2} x_{i3} + d_i, \\ \dot{x}_{i3} &= f_{i3}(\bar{x}_{i3}) + g_{i3} Q(u_i) \\ &\quad + h_i(x_{i1}, x_{j1\tau}(t-\tau_{j/i}), x_{j2\tau}(t-\tau_{j/i})) \\ y_{i1} &= x_{i1}, \end{aligned} \tag{12}$$

$$\begin{aligned} \dot{x}_{i4} &= g_{i4} Q\left(u'_{Bi}\right) + f_{i4}(\bar{x}_{i4}), \\ y_{i2} &= x_{i4}, \end{aligned} \tag{13}$$

where y_{i1} and y_{i2} are the outputs of multi-machine power systems and the SVC equipments, respectively; $\bar{x}_{il} = [x_{i1}, \cdots, x_{il}]^T$, $i = 1, \cdots, n$, $l = 2, \cdots, 4$, $f_{i2}(\bar{x}_{i2}) = -\frac{D_i}{2H_i} x_{i2}$, $f_{i3}(\bar{x}_{i3}) = -\frac{1}{T'_{doi}} x_{i3}$, $g_{i2} = \frac{\omega_0}{2H_i}$, $g_{i3} = \frac{1}{T'_{doi}}$, $g_{i4} = \frac{X_{1i}X_{2i}}{T_{\mathrm{Ci}} X'_{d\Sigma i}}$, $u'_{Bi} = -x_{i4} u_{Bi}$ with u_{Bi} being the input signal of SVC equipment,

$$\begin{aligned} f_{i4}(\bar{x}_{i4}) = &-\frac{\sin x_{i1} X_{1i} X_{2i}}{\left(x_{i4} + V_{refi}\right)\left(X'_{d\Sigma i}\right)^2} x_{i2} E'_{qi} \\ &- \frac{X_{1i}X_{2i}\left(x_{i4} + V_{refi}\right)}{X'_{d\Sigma i}} \frac{1}{T_{ci}} \left(-B_{Li} + B_{\mathrm{Ci}}\right) \\ &+ \frac{X_{2i}^2 E'_{qi} + X_{1i}X_{2i}\cos x_{i1}}{\left(x_{i4} + V_{refi}\right)\left(X'_{d\Sigma i}\right)^2} \\ &\times \left(-\frac{X_{d\Sigma i}}{T_{doi} X'_{d\Sigma i}} E'_{qi} + \frac{1}{T_{doi}} \frac{X_{di} - X'_{di}}{X'_{d\Sigma i}} \cos x_{i1}\right) \\ &+ \frac{X_{2i}^2 x_{i3} + X_{1i}X_{2i} V_{si} \cos \delta_i}{T_{doi} V_{mi} \left(X'_{d\Sigma i}\right)^2} u_i \end{aligned}$$

with $X_{d\Sigma i} = X_{3i} + X_{2i} + X_{3i}X_{2i}(B_{Li} - B_{\mathrm{Ci}})$, $X_{3i} = x_{di} + X_{Ti}$.

To proceed, the following assumptions and Lemma are necessary:

A1: The reference signal y_{ri} are smooth and bounded functions with $y_{ri}(0)$ at a designer's disposal; $[y_{ri}, \dot{y}_{ri}, \ddot{y}_{ri}]^T$ belongs to a compact set Ω_r for all $t \ge 0$.

A2: There exists some positive constants $g_{\min}$ and $g_{\max}$ such that $g_{\min} \le g_{ij} \le g_{\max}$, $i = 1, 2, \cdots, n$, $j = 2, 3$.

Lemma 1 [35], [36]: Suppose $f(x) : \Omega_x \subset \mathbb{R}$ be a smooth function with $\Omega_x \subset \mathbb{R}^n$ being a compact set. Let $x(t-\tau)$ be uniformly continuous with respect to t, where $\tau \in [0, \tau_m]$ is an unknown constant time delay with τ_m denoting the maximum value of τ. Then, for any given $\delta_0 > 0$, there exists a finite partition of $[0, \tau_m]$, independent of t, $0 \le t_1 < t_2 < \cdots < t_k \le \tau_m$, from which a point $\bar{\tau} \in \{t_1, \cdots, t_k\}$, can be extracted, such that $|f(x(t-\tau)) - f(x(t-\bar{\tau}))| < \delta_0$, $\forall t \ge 0$.

Remark 1: Since the reference signal y_{ri} is always bounded and $g_{i,j}$, $j = 2, 3$ are unknown positive constants, the assumption A1 and A2 are reasonable [36]–[39].

D. RADIAL BASIS FUNCTION NEURAL NETWORKS (RBFNNS)

The RBFNNs in [40] are used as the continuous functional approximator with the following form

$$f_{ij}\left(\xi_{ij}\right) = \vartheta_{ij}^{*T}\psi_{ij}\left(\xi_{ij}\right) + \varepsilon_{ij}\left(\xi_{ij}\right), \tag{14}$$

where $f_{ij}\left(\xi_{ij}\right)$ are continuous functions, $\xi_{ij} \in R^n$ are the inputs of RBFNNs; $\vartheta_{ij}^* \in R^M$ is an M-dimensional optimal weight vector with M being the number of the neural nodes, satisfying $\vartheta_{ij}^* = \arg\min_{\vartheta \in R^M}\left\{\sup_{\xi \in \Omega_\xi}\left|\vartheta_{ij}^{*T}\psi_{ij}\left(\xi_{ij}\right) - f_{ij}\left(\xi_{ij}\right)\right|\right\}$; $\psi_{ij}\left(\xi_{ij}\right) : R^n \rightarrow R^M$ is nonlinear vector function and $\psi_{ij}\left(\xi_{ij}\right) = \left[\psi_{ij,1}\left(\xi_{ij}\right), \cdots, \psi_{ij,M}\left(\xi_{ij}\right)\right]^T$; $\psi_{ij,k}\left(\xi_{ij}\right)$, is the basis function called Gauss function with $\psi_{ij,k}\left(\xi_{ij}\right) = \exp\left(-\frac{\|\xi_{ij}-\zeta_{ij,k}\|^2}{2\eta_{ij}^2}\right)$, ζ_j, $k = 1, \ldots, M$, being the center of the basis functions; η_{ij} denotes the width of the basis functions; $\varepsilon_{ij}\left(\xi_{ij}\right)$ is the approximation error satisfying

$$\left|\varepsilon_{ij}\left(\xi_{ij}\right)\right| \leq \varepsilon_{ijm} \tag{15}$$

with $\varepsilon_{im} > 0$ being the maximum vale of $\varepsilon_{ij}\left(\xi_{ij}\right)$.

The control objective is to propose a neural decentralized adaptive quantized dynamic surface excitation control scheme for a class of large-scale multi-machine power systems with SVC such that the power angles, the speed, the electrical power and the accessing voltage of the SVC converge to desired values with the $\mathcal{L}_\infty$ norm of the tracking error even if the large-scale power systems encounter the unexpected disturbances and all the signals of the closed-loop system are ultimately uniformly bounded.

III. DESIGN PROCEDURES OF THE DECENTRALIZED NEURAL ADAPTIVE QUANTIZED DYNAMIC SURFACE CONTROL (QDSC)

In this section, the dynamic surface (DSC) technique will be employed for the controller design. Because each subsystem (10) is third-order, three steps are needed based on the rules of DSC technique. Similarly, because each subsystem (11) is first-order, only one step is needed. Therefore, four steps are included in the procedures of the controller design as follows.

Step 1: Let s_{i1} be the first surface error and defined as

$$s_{i1} = x_{i1} - y_{ri}. \tag{16}$$

Then, the time derivative of s_{i1} yields

$$\dot{s}_{i1} = x_{i2} - \dot{y}_{ri}. \tag{17}$$

Consider the following quadratic function

$$V_1 = \frac{1}{2}\sum_{i=1}^{n} s_{i1}^2. \tag{18}$$

Then, the time derivative of V_1 can be expressed as

$$\dot{V}_1 = \sum_{i=1}^{n} s_{i1}\left[\left(x_{i2} - x_{2di}\right) - \dot{y}_{ri} + x_{2di}\right] \tag{19}$$

with x_{2di} being the virtual control signal to be designed. From (19), the virtual control law is suggested to choose as

$$x_{2di} = -k_{i1}s_{i1} + \dot{y}_{ri}, \tag{20}$$

where k_{i1} is positive design parameter.

Let x_{2di} pass through a first-order low pass filter, a new variable z_{i2} can be obtained as follows.

$$\varkappa_{i2}\dot{z}_{i2} + z_{i2} = x_{2di} \tag{21}$$

with $\varkappa_{i2}$ being a time constant of the low pass filter.

Step 2: Let s_{i2} be the second surface error and defined as

$$s_{i2} = x_{i2} - z_{i2} - c_{i2} \tag{22}$$

with c_{i2} being a constant design parameter to guarantee the $\mathcal{L}_\infty$ performance. Consider the following quadratic function

$$V_2 = \sum_{i=1}^{n}\left(\frac{1}{2g_{i2}}s_{i2}^2 + \frac{1}{2\gamma_{i2}}\tilde{\nu}_{i2}^2\right), \tag{23}$$

where $\tilde{\nu}_{i2} = \hat{\nu}_{i2} - \nu_{i2}^*$ with $\hat{\nu}_{i2}$ being the estimation of ν_{i2}^* which will be defined below. Then, the time derivative of V_2 yields

$$\dot{V}_2 = \sum_{i=1}^{n}[s_{i2}(-x_{i3} + \frac{1}{g_{i2}}\left(f_{i2}\left(\bar{x}_{i2}\right) + d_i - \dot{z}_{i2}\right)) + \frac{1}{\gamma_{i2}}\tilde{\nu}_{i2}\dot{\hat{\nu}}_{i2}], \tag{24}$$

where γ_{i2} is a positive design parameter.

Here, the RBFNNs is employed to approximate the unknown continuous functions on the compact sets $\Omega_{\xi i2}$ as follows.

$$\frac{1}{g_{i2}}(f_{i2}\left(\bar{x}_{i2}\right) + d_i - \dot{z}_{i2}) + \frac{3}{2}s_{i2} = \vartheta_{i2}^{*T}\psi_{i2}\left(\xi_{i2}\right) + \varepsilon_{i2}\left(\xi_{i2}\right) \tag{25}$$

with ϑ_{i2}^* being the optimal weighted vector as in (14), $\xi_{i2} = \left(x_{i1}, x_{i2}, z_{i2}\right) \in \Re^3$, $\left|\varepsilon_{i2}\left(\xi_{i2}\right)\right| \leq \varepsilon_{i2m}$. Let $\nu_{i2}^* = \left\|\vartheta_{i2}^{*T}\right\|^2$. By using the Young's inequalities, it follows that

$$s_{i2}\vartheta_{i2}^{*T}\psi_{i2}\left(\xi_{i2}\right) \leq \frac{\alpha_{i2}^2\nu_{i2}^*\psi_{i2}^T\psi_{i2}s_{i2}^2}{2} + \frac{1}{2\alpha_{i2}^2}, \tag{26}$$

$$s_{i2}\varepsilon_{i2}\left(\xi_{i2}\right) \leq \frac{1}{2}s_{i2}^2 + \frac{1}{2}\varepsilon_{i2m}^2 \tag{27}$$

with α_{i2} being a positive design parameter and ε_{i2m} denoting the upper boundary of the approximation error described in (15).

Substituting (25)-(27) into (24), it follows that

$$\begin{aligned}\dot{V}_2 \leq \sum_{i=1}^{n}[&s_{i2}(-\left(x_{i3} - x_{3di}\right) - x_{3di} \\ &+ \frac{\alpha_{i2}^2\nu_{i2}^*\psi_{i2}^T\psi_{i2}s_{i2}}{2}) - \frac{1}{2}s_{i2}^2 + \frac{1}{2}\varepsilon_{i2m}^2 \\ &+ \frac{1}{2\alpha_{i2}^2} + \frac{1}{\gamma_{i2}}\tilde{\nu}_{i2}\dot{\hat{\nu}}_{i2}]\end{aligned} \tag{28}$$

with x_{3di} being the virtual control signal to be designed. From (28), the virtual control law is suggested to choose as

$$x_{3di} = k_{i2}s_{i2} + \frac{\alpha_{i2}^2 \hat{\nu}_{i2}\psi_{i2}^T\psi_{i2}s_{i2}}{2} \tag{29}$$

with k_{i2} being a positive design parameter. Then, the adaptive law for the estimation of the unknown parameter ν_{i2}^* is designed as

$$\dot{\hat{\nu}}_{i2} = \gamma_{i2}\left(\frac{\alpha_{i2}^2\psi_{i2}^T\psi_{i2}s_{i2}^2}{2} - \sigma_{i2}\hat{\nu}_{i2}\right), \tag{30}$$

where γ_{i2} and σ_{i2} are positive design parameters.

Let x_{3di} pass through the first-order low pass filter to generate a new variable z_{i3}.

$$\varkappa_{i3}\dot{z}_{i3} + z_{i3} = x_{3di} \tag{31}$$

with $\varkappa_{i3}$ being a time constant of the low pass filter.

Step 3: Let s_{i3} be the third surface error and defined as

$$s_{i3} = x_{i3} - z_{i3} - c_{i3} \tag{32}$$

with c_{i3} being a constant design parameter similar as c_{i2} defined in (22). Then, the time derivative of s_{i3} yields

$$\begin{aligned}\dot{s}_{i3} = g_{i3}[&Q(u_i) + \frac{1}{g_{i3}}(f_{i3}(\bar{x}_{i3}) \\ &+ h_i\left(x_{i1}, x_{j1}\left(t-\tau_j\right), x_{j2}(t-\tau_j)\right) - \dot{z}_{i3})].\end{aligned} \tag{33}$$

With respect to $Q(u_i)$, define

$$\iota_{i1}(t) = \begin{cases}\dfrac{Q(u_i)}{u_i}, & \text{if } |u_i| \geq a(t),\\ 1, & \text{if } |u_i| < a(t),\end{cases} \tag{34}$$

$$\iota_{i2}(t) = \begin{cases}0, & \text{if } |u_i| \geq a(t),\\ Q(u_i) - u_i, & \text{if } |u_i| < a(t),\end{cases} \tag{35}$$

where $a(t)$ is defined in (11). Then, it follows that

$$Q(u_i) = \iota_{i1}(t)u_i + \iota_{i2}(t). \tag{36}$$

From FIGURE 1, it arrives at

$$1 - \delta \leq \frac{Q(u_i)}{u_i} \leq 1 + \delta, \quad \text{if } |u_i| \geq a(t), \tag{37}$$

$$|Q(u_i) - u_i| < a, \quad \text{if } |u_i| < a(t). \tag{38}$$

Considering (37), (38), (11) and the relationship $\delta_i = \frac{1-\epsilon_i}{1+\epsilon_i}$, one has

$$\iota_{i1}(t) \geq \lambda_i, \quad \iota_{i2}(t) \leq \bar{a}, \ \forall t \geq 0, \tag{39}$$

where $\lambda_i > 0$, satisfies

$$\lambda_i = \frac{2\epsilon_{i\min}}{1+\epsilon_{i\min}}. \tag{40}$$

From Lemma 1, there exists a point $\tau_{ej/i} \subset \{t_1, \cdots, t_m\}$, $j = 1, ..n$, such that $h_i\left(x_{i1}, x_{j1\tau}\left(t-\tau_{j/i}\right)\right.$, $x_{j2\tau}\left(t-\tau_{j/i}\right)\big) = h_i\left(x_{i1}, x_{j1}\left(t-\tau_{ej/i}\right), x_{j2}\left(t-\tau_{ej/i}\right)\right) + e_i$ with $|e_i| \leq \delta_{i0}$. Then, (33) can be rewritten as

$$\begin{aligned}&\sum_{i=1}^{n} s_{i3}\dot{s}_{i3} \\ &\leq \sum_{i=1}^{n} g_{i3}s_{i3}[u_i + \frac{1}{g_{i3}}(f_{i3}(\bar{x}_{i3}) - \dot{z}_{i3} + e_i \\ &\quad + \sum_{j=1}^{n}(\gamma_{i1j}(\left|x_{j1}\left(t-\tau_{ej/i}\right)\right|) + \gamma_{i2}\left|x_{j2}\left(t-\tau_{ej/i}\right)\right|)]\end{aligned} \tag{41}$$

holds. Noted that,

$$\begin{aligned}&\sum_{i=1}^{n}\sum_{j=1}^{n}(\gamma_{i1j}(\left|x_{j1}\left(t-\tau_{ej/i}\right)\right|) + \gamma_{i2}\left|x_{j2}\left(t-\tau_{ej/i}\right)\right|) \\ &\qquad = \sum_{i=1}^{n}\sum_{j=1}^{n}(\gamma_{j1i}(\left|x_{i1}\left(t-\tau_{ei/j}\right)\right|) + \gamma_{j2}\left|x_{i2}\left(t-\tau_{ei/j}\right)\right|).\end{aligned}$$

Then, similar to Step 2, the RBFNNs are utilized to approximate the unknown continuous functions on the compact set $\Omega_{\xi i3}$ as follows

$$\begin{aligned}&\frac{1}{g_{i3}}f_{i3}(\bar{x}_{i3}) - \dot{z}_{i3} + \frac{1}{2g_{i3}}s_{i3} \\ &\quad + \sum_{j=1}^{n}(\gamma_{j1i}(\left|x_{i1}\left(t-\tau_{ei/j}\right)\right|) + \gamma_{j2}\left|x_{i2}\left(t-\tau_{ei/j}\right)\right|) \\ &= \vartheta_{i3}^{*T}\psi_{i3}(\xi_{i3}) + \varepsilon_{i3}(\xi_{i3})\end{aligned} \tag{42}$$

with ϑ_{i3}^* being the optimal weighted vector as in (14), and

$$\begin{aligned}\xi_{i3} = (&x_{i1}, x_{i2}, x_{i3}, x_{i1}(t-t_1), \ldots, x_{i1}(t-t_m), \\ &x_{i2}(t-t_1), \ldots, x_{i2}(t-t_m), z_{i3}) \in \Re^{4+2m}.\end{aligned}$$

Consider the following quadratic function

$$V_3 = \sum_{i=1}^{n}\left(\frac{1}{2g_{i3}}s_{i3}^2 + \frac{1}{2\gamma_{i3}}\tilde{\nu}_{i3}^2 + \frac{\lambda_i}{2\gamma_\iota}\tilde{\iota}_i^2\right), \tag{43}$$

where $\tilde{\nu}_{i3} = \hat{\nu}_{i3} - \nu_{i3}^*$ and $\tilde{\iota}_i = \hat{\iota}_i - \iota_i^*$ with $\hat{\nu}_{i3}$ and $\hat{\iota}_i$ being the estimations of ν_{i3}^* and $\iota_i^* = \frac{1}{\lambda_i}$, respectively. Then, substitute (42) into (41), it follows that

$$\begin{aligned}s_{i3}\dot{s}_{i3} \leq g_{i3}[&s_{i3}(\iota_{i1}(t)u_i + \iota_{i2}(t) + \frac{\alpha_{i3}^2\nu_{i3}^*\psi_{i3}^T\psi_{i3}s_{i3}}{2}) \\ &+ \frac{1}{2}\varepsilon_{i3m}^2 + \frac{1}{2\alpha_{i3}^2} + \frac{1}{2}\delta_{i0}^2].\end{aligned} \tag{44}$$

Let $\nu_{i3}^* = \left\|\vartheta_{i3}^{*T}\right\|^2$, and using the Young's inequalities, we have

$$s_{i3}e_i \leq \frac{1}{2}s_{i3}^2 + \frac{1}{2}\delta_{i0}^2, \tag{45}$$

$$s_{i3}\vartheta_{i3}^{*T}\psi_{i3}(\xi_{i3}) \leq \frac{\alpha_{i3}^2\nu_{i3}^*\psi_{i3}^T\psi_{i3}s_{i3}^2}{2} + \frac{1}{2\alpha_{i3}^2}, \tag{46}$$

$$s_{i3}\varepsilon_{i3}(\xi_{i3}) \leq \frac{1}{2}s_{i3}^2 + \frac{1}{2}\varepsilon_{i3m}^2 \tag{47}$$

with α_{i3} being a positive design parameter and ε_{i3m} being the upper boundary of the approximation error. Then, the time derivative of V_3 yields

$$\dot{V}_3 \leq \sum_{i=1}^{n}[s_{i3}(\iota_{i1}(t)u_i + \iota_{i2}(t) + \frac{\alpha_{i3}^2 \nu_{i3}^* \psi_{i3}^T \psi_{i3} s_{i3}}{2}) + \frac{1}{2}\varepsilon_{i3m}^2 + \frac{1}{2\alpha_{i3}^2} + \frac{1}{2}\delta_{i0}^2 + \frac{1}{\gamma_{i3}}\tilde{\nu}_{i3}\dot{\hat{\nu}}_{i3} + \frac{1}{\gamma_\iota}\tilde{\iota}_i\dot{\hat{\iota}}_i] \quad (48)$$

To stabilize each subsystem, the actual control laws u_i are chosen as

$$u_i = -\frac{s_{i3}\bar{\nu}_{i1}^2}{|s_{i3}\bar{\nu}_i| + \varrho_{i1}}, \quad (49)$$

where ϱ_{i1} is a positive design parameter.

$$\bar{\nu}_{i1} = \hat{\iota}_i \bar{\nu}_{i1}', \quad (50)$$

and

$$\bar{\nu}_{i1}' = -k_{i3}s_{i3} - \frac{\alpha_{i3}^2 \hat{\nu}_{i3}\psi_{i3}^T\psi_{i3}s_{i3}}{2} \quad (51)$$

with k_{i3} being a design parameters. The adaptive laws for the unknown parameter ν_{i3}^* and $\hat{\iota}_i$ are selected as

$$\dot{\hat{\nu}}_{i3} = \gamma_{i3}\left(\frac{\alpha_{i3}^2\psi_{i3}^T\psi_{i3}s_{i3}^2}{2} - \sigma_{i3}\hat{\nu}_{i3}\right), \quad (52)$$

$$\dot{\hat{\iota}}_i = \gamma_\iota\left(s_{i3}\bar{\nu}_i' - \sigma_\iota\hat{\iota}_i\right), \quad (53)$$

where γ_{i3}, γ_ι σ_{i3}, and σ_ι are positive design parameters.

Step 4: Let s_{i4} be the third surface error and defined as

$$s_{i4} = x_{i4} - V_{refi}, \quad (54)$$

where s_{i4} denotes the tracking error between the accessing point voltage V_{mi} and the reference voltage V_{refi} in SVC. Then the time derivative of s_{i4} yields

$$\dot{s}_{i4} = g_{i4}Q\left(u_{Bi}'\right) + f_{i4}(\bar{x}_{i4}) - \dot{V}_{refi}. \quad (55)$$

Similar to (34)-(40), one has

$$Q\left(u_{Bi}'\right) = \iota_{i3}(t)u_{Bi}' + \iota_{i4}(t) \quad (56)$$

with

$$\iota_{i3}(t) = \begin{cases} \dfrac{Q\left(u_{Bi}'\right)}{u_{Bi}'}, & \text{if } \left|u_{Bi}'\right| \geq a(t), \\ 1, & \text{if } \left|u_{Bi}'\right| < a(t), \end{cases} \quad (57)$$

$$\iota_{i4}(t) = \begin{cases} 0, & \text{if } \left|u_{Bi}'\right| \geq a(t), \\ Q\left(u_{Bi}'\right) - u_{Bi}', & \text{if } \left|u_{Bi}'\right| < a(t). \end{cases} \quad (58)$$

Consider the following quadratic function

$$V_4 = \sum_{i=1}^{n}\left(\frac{1}{2g_{i4}}s_{i4}^2 + \frac{1}{2\gamma_{i4}}\tilde{\nu}_{i4}^2 + \frac{\lambda_i}{2\gamma_\iota'}\tilde{\iota}_i^2\right) \quad (59)$$

where $\tilde{\nu}_{i4} = \hat{\nu}_{i4} - \nu_{i4}^*$ and $\tilde{\iota}_i' = \hat{\iota}_i' - \iota_i'^*$, with $\hat{\nu}_{i4}$ and $\hat{\iota}_i'$ being the estimations of ν_{i4}^* and $\iota_i^* = \frac{1}{\lambda_i'}$, respectively and will be introduced below. Then, time derivative of V_4 is

$$\dot{V}_4 = \sum_{i=1}^{n}\left(s_{i4} - \frac{1}{g_{i4}}\dot{V}_{refi} + \frac{f_{i4}(\bar{x}_{i4})}{g_{i4}} + [\iota_{i3}(t)u_{i4} + \iota_{i4}(t) + \frac{1}{\gamma_{i4}}\tilde{\nu}_{i4}\dot{\hat{\nu}}_{i4} + \frac{1}{\gamma_\iota'}\tilde{\iota}_i'\dot{\hat{\iota}}_i'\right). \quad (60)$$

Then, similar to Step 2 and Step 3, the RBFNNs are utilized to approximate the unknown continuous functions on the compact set $\Omega_{\xi i4}$ as follows

$$\frac{1}{g_{i4}}\left[f_{i4}(\bar{x}_{i4}) - \dot{V}_{refi}\right] + \frac{1}{2}s_{i4} = \vartheta_{i4}^{*T}\psi_{i4}(\xi_{i4}) + \varepsilon_{i4}(\xi_{i4}) \quad (61)$$

with $\xi_{i4} = \left(\bar{x}_{i4}, \varpi_{i2}, \dot{\varpi}_{i2}, e_{i2}, \dot{V}_{refi}\right) \in \Omega_{\xi i4} \subset \Re^8$. Let $\nu_{i4}^* = \left\|\vartheta_{i4}^{*T}\right\|^2$ and using the Young's inequalities, we obtain

$$s_{i4}\vartheta_{i4}^{*T}\psi_{i4}(\xi_{i4}) \leq \frac{\alpha_{i4}^2\nu_{i4}^*\psi_{i4}^T\psi_{i4}s_{i4}^2}{2} + \frac{1}{2\alpha_{i4}^2}, \quad (62)$$

$$s_{i4}\varepsilon_{i4}(\xi_{i4}) \leq \frac{1}{2}s_{i4}^2 + \frac{1}{2}\varepsilon_{i4m}^2 \quad (63)$$

with α_{i4} being a positive design parameter and ε_{i4m} being the upper boundary of the approximation error. Substituting (61)-(63) into (60), it follows that

$$\dot{V}_4 \leq \sum_{i=1}^{n}s_{i4}\left[\left(\iota_{i3}(t)u_{Bi}' + \iota_{i4}(t)\right) + \frac{\alpha_{i4}^2\nu_{i4}^*\psi_{i4}^T\psi_{i4}s_{i4}}{2}\right] + \frac{1}{2}\varepsilon_{i4m}^2 + \frac{1}{2\alpha_{i4}^2} + \frac{1}{\gamma_{i4}}\tilde{\nu}_{i4}\dot{\hat{\nu}}_{i4} + \frac{1}{\gamma_\iota'}\tilde{\iota}_i'\dot{\hat{\iota}}_i'. \quad (64)$$

Then, the control law for the accessing point voltage of SVC and the adaptive laws for the estimations of $\hat{\nu}_{i4}$ and $\hat{\iota}_i'$ are chosen as follows

$$u_{Bi}' = -\frac{s_{i4}\bar{\nu}_{i2}^2}{|s_{i4}\bar{\nu}_{i2}| + \varrho_{i2}}, \quad (65)$$

where ϱ_{i2} is a positive design parameter and

$$\bar{\nu}_{i2} = \hat{\iota}_i'\bar{\nu}_{i2}', \quad (66)$$

$$\bar{\nu}_{i2}' = -k_{i4}s_{i4} - \frac{\alpha_{i4}^2\hat{\nu}_{i4}\psi_{i4}^T\psi_{i4}s_{i4}}{2}, \quad (67)$$

$$\dot{\hat{\nu}}_{i4} = \gamma_{i4}\left(\frac{\alpha_{i4}^2\psi_{i4}^T\psi_{i4}s_{i4}^2}{2} - \sigma_{i4}\hat{\nu}_{i4}\right), \quad (68)$$

$$\dot{\hat{\iota}}_i' = \gamma_\iota'\left(s_{i3}\bar{\nu}_{i4}' - \sigma_\iota'\hat{\iota}_i'\right) \quad (69)$$

with k_{i4}, γ_{i4}, γ_ι', σ_ι' and σ_{i4} are positive design parameters.

Remark 2: It should be noted that the utilization of the design parameters c_{ij} in (22) and (32) guarantees the arbitrarily small $\mathcal{L}_\infty$ performance of the tracking error as shown in the next section. Here, the arbitrarily small $\mathcal{L}_\infty$ performance implies the norms of the tracking errors of each generator $\sup_{t>0}\|S_{i1}\|_\infty$ can be arbitrarily small for all $t > 0$, by properly choosing the design parameters. Obviously, the

$\mathcal{L}_\infty$ performance of the tracking error improves tracking performance of the control systems compared with the traditional backstepping methods [13], [40]–[44].

Remark 3: In this paper, the norms of M-dimensional optimal weight vectors, such as ν_{i2}^*, ν_{i3}^* and ν_{i4}^* with M being the number of neural nodes, are estimated. Therefore, the number of the estimated unknown neural nodes is dramatically reduced from M to only one, leading to the computational burden being greatly reduced and the proposed method are more suitable for real time control compared with [43] and [44].

Remark 4: It should be noted that the objective of this paper is not to use RBFNNs to exactly approximate the unknown continuous functions (25), (42) and (61), but to make the output of the control system precisely tracks the desired trajectory or in other word, to make the tracking error of the control system satisfies the desired requirement. It implies that if the tracking error of the control system is bigger than the desired requirement, the design parameters γ_{i2}, γ_{i3}, γ_{i4}, σ_{i2}, σ_{i3}, σ_{i4}, in the adaptive laws (30), (52) and (68) can be changed. Then, the on-line estimation values of the norm of NNs weights vectors will be updated.

Remark 5: When the time delay functions are approximate by RBFNNs, the time-delay states $x_{ij}(t-t_1), \cdots, x_{ij}(t-t_k)$ are used as the input vector of RBFNNs, where $t_1, \cdots, t_k$ is a finite partition of $[0, \tau_m]$ satisfying $0 \le t_1 < t_2 < \cdots < t_k \le \tau_m$ as shown in Lemma 1. Fortunately, we do not need to memory all the previous states, only very limitedly previous states are needed with respect to the current time t, which implies if $k = 10$, only 10 states are needed to be stored with respect to the current time. Therefore, the time-delay approximator may not lead to the requirement of unacceptable storage space.

Remark 6: To make the proposed dynamic surface control scheme more implementable, the design parameters could be chosen as the following steps. Firstly, the time constants of the first-order low-pass filters $\varkappa_{ij}$, $i = 1, 2; j = 2, 3$, should be chosen a smaller value within the practically allowable range from 0.001 to 0.1. Secondly, when the value of B_{i0} is selected by using (93), the value of α_{i0} could be chosen according to (101) and (102). Thirdly, by using the value of α_{i0} obtained in Step 2 and according to (105), the design parameters k_{i1}, k_{i2}, k_{i3}, k_{i4}, γ_{i2}, γ_{i3}, γ_{i4}, γ_ι, $\gamma_{\iota'}$, σ_{i2}, σ_{i3}, σ_{i4}, σ_ι, and $\sigma_{\iota'}$ could be chosen.

IV. ANALYSIS OF STABILITY AND TRACKING PERFORMANCE

In this section, the analysis of stability for the multi-machine power systems and the tracking performance of power angles will be presented. To this end, define y_{i2e} and y_{i3e} as follows.

$$\begin{aligned} y_{i2e} &= z_{i2} - x_{2di} \\ &= z_{i2} - (-k_{i1}s_{i1} + \dot{y}_{ri} - s_{i1}), \end{aligned} \tag{70}$$

$$\begin{aligned} y_{i3e} &= z_{i3} - x_{3di} \\ &= z_{i2} - \left(k_{i2}s_{i2} + \frac{\alpha_{i2}^2 \hat{\nu}_{i2}\psi_{i2}^T\psi_{i2}s_{i2}}{2}\right) \end{aligned} \tag{71}$$

with x_{2di} and x_{3di} being given by (20) and (29), respectively. From (21) and (70), we have

$$\dot{z}_{i2} = \frac{x_{2di} - z_{i2}}{\varkappa_{i2}} = \frac{-y_{i2e}}{\varkappa_{i2}}. \tag{72}$$

Similarly, from (31) and (71), one has

$$\dot{z}_{i3} = \frac{x_{3di} - z_{i3}}{\varkappa_{i3}} = \frac{-y_{i3e}}{\varkappa_{i3}}. \tag{73}$$

Then, the time derivatives of (70) and (71) arrive at

$$\dot{y}_{i2e} = \frac{-y_{i2e}}{\varkappa_{i2}} + B_{i2}\left(s_{i1}, s_{i2}, y_{i2e}, \dot{y}_{ri}, \ddot{y}_{ri}\right), \tag{74}$$

$$\begin{aligned} \dot{y}_{i3e} = {} & \frac{-y_{i3e}}{\varkappa_{i3}} + B_{i3}(s_{i1}, s_{i2}, s_{i3}, y_{i2e}, y_{i3e}, \\ & \hat{\nu}_{i2}, \varpi_{i1}, \dot{\varpi}_{i1}, \ddot{\varpi}_{i1}, y_{ri}, \dot{y}_{ri}, \ddot{y}_{ri}), \end{aligned} \tag{75}$$

where

$$B_{i2} = k_{i1}\dot{s}_{i1} - \ddot{y}_{ri} + \dot{s}_{i1}, \tag{76}$$

$$\begin{aligned} B_{i3} = {} & -[k_{i2}\dot{s}_{i2} + \frac{\alpha_{i2}^2\hat{\nu}_{i2}\psi_{i2}^T\psi_{i2}\dot{s}_{i2}}{2} \\ & + \frac{\alpha_{i2}^2\dot{\hat{\nu}}_{i2}\psi_{i2}^T\psi_{i2}s_{i2}}{2} \\ & + \alpha_{i2}^2\hat{\nu}_{i2}\psi_{i2}^T s_{i2}(\sum_{i=1}^{2}\frac{\partial\psi_{i2}}{\partial x_l}\dot{x}_{il} + \frac{\partial\psi_{i2}}{\partial s_{i2}})], \end{aligned} \tag{77}$$

are continuous functions.

Theorem 1: Consider the closed-loop control systems including the transformed multi-machine power systems with SVC and transmission time delays, hysteresis quantizer (10), first-order low-pass filters (21), (31), actual control law (65), and adaptive laws (30) (52)and (68). The positive definite Lyapunov function are defined as

$$V = \sum_{i=1}^{4} V_i + \frac{1}{2}\sum_{i=1}^{n} y_{i2e}^2 + \frac{1}{2}\sum_{i=1}^{n} y_{i3e}^2 \tag{78}$$

with V_1, V_2, V_3 and V_4 being defined in (18), (23), (43) and (59), respectively. Suppose that the given positive constant ε_{ilm} in (27) and (47) satisfied $|\varepsilon_{il}(\xi_{il})| \le \varepsilon_{ilm}$, $l = 2, 3, 4$, in the compact set $\Omega_{\xi i2}$, $\Omega_{\xi i3}$, and $\Omega_{\xi i4}$, respectively. For the bounded initial conditions and a given positive constant p, if

$$V(0) \le p, \tag{79}$$

then, all the variables such as s_{i1}, s_{i2}, s_{i3}, s_{i4}, ν_{i2}, ν_{i3}, ν_{i4}, in the closed-loop systems are ultimately uniformly bounded by appropriately choosing the design parameters k_{i1}, k_{i2}, k_{i3}, k_{i4}, γ_{i2}, γ_{i3}, γ_{i4}, γ_ι, $\gamma_{\iota'}$, σ_{i2}, σ_{i3}, σ_{i4}, σ_ι and $\sigma_{\iota'}$. Also, the controlled power system can adaptively and promptly return to stability when it encounters the unexpected faults. In addition, the $\mathcal{L}_\infty$ norm of the tracking errors of the power angles can be arbitrarily small by properly choosing the above design parameters.

Proof: please see the APPENDIX for the details.

Remark 7: As shown in [45], when the NNs is used to approximate the unknown nonlinear function in an adaptive

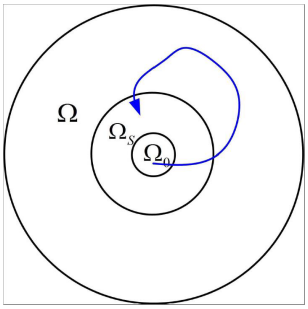

FIGURE 2. The relationship among the three compacts.

control scheme, there are three compact sets: initial compact set $\Omega_0 = \{V(0), y_r(0) \,|V(0)$ is finite, $y_r(0) \in \Omega_r\}$, bounding compact set $\Omega = \{V(t) \,|V(t) \leq p\}$, where p can be sufficient large value defined in (79), and the steady state compact $\Omega_S = \{V(t) \left| \lim_{t\to\infty} \|x_{i1} - y_{ri}\| \leq \sqrt{\frac{C^*}{\alpha_{i0}}}\}$, where C^* and α_{i0} defined in (104) and (105), respectively. The relationship among the three compact sets is illustrated in FIGURE 2. Therefore, with respect to the compact set over the NNs approximations $\Omega_{\xi_{i2}}$, $\Omega_{\xi_{i3}}$, and $\Omega_{\xi_{i2}}$, stable adaptive neural network controllers can be easily constructed if the compact sets over the NNs approximations are chosen large enough to cover for bounded initial conditions [45].

Remark 8: For the control system, the norm of weight vector $\upsilon_{ij}^* = \left\|\vartheta_{ij}^*\right\|^2$ is estimated instead of the weight vector itself and the estimated norms of optimal weight vector are updated on-line by using the adaptive laws (30), (52) and (68). According to (30), (52) and (68), the different choices of neural network basis functions and number of neurons lead to different estimated values $\hat{\upsilon}_{ij}$, different values of approximation error ε_{ij} and its corresponding maximum value of ε_{ijm}. The larger values of approximation error will make the value of C^* in (105) become larger, then, the tracking error s_{i1} and s_{i4} become larger due to (118). Generally, the larger number of neurons leads to the smaller approximation error when the same neural network basis functions are chosen.

Remark 9: By using the proposed control scheme, the Krasovskii functions in [14] and [15] that are used to deal with time delays and the conservative assumptions of upper bound functions on the time delay functions have been totally abandoned. This leads to the achievement of the arbitrarily small $\mathcal{L}_\infty$ norm of the tracking error as shown in this paper. On the contrary, the utilization of Krasovskii functions makes it impossible to obtain the arbitrarily small $\mathcal{L}_\infty$ norm of the tracking error due to the existence of the Krasovskii functions in transient performance analysis.

The design parameters of virtual control laws and final control laws are selected as $k_{11} = 3.2$, $k_{21} = 4.2$; $k_{12} = 2$, $k_{22} = 4, 3$; $k_{13} = 5$, $k_{23} = 4.5$; $k_{14} = 5.1$, $k_{24} = 4.3$; the time constants of the low-pass filter at each step are selected as $\varkappa_{12} = \varkappa_{22} = 0.005$, $\varkappa_{13} = \varkappa_{23} = 0.01$; the design parameters of the adaptive laws are selected as $r_{12} = 3$, $\sigma_{12} = 0.001$; $r_{13} = 3$, $\sigma_{23} = 0.0005$; $r_{14} = 5$, $\sigma_{24} = 0.0001$.

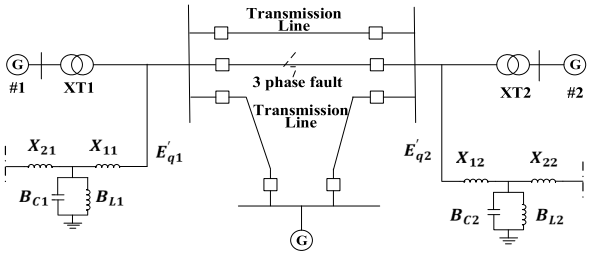

FIGURE 3. Two-machine excitation systems with SVC equipment.

TABLE 2. System parameters of the two-machine excitation systems with SVC equipment.

	Generator#1	Generator#2
$x_d\,(p.u.)$	1.863	2.36
$\acute{x}_d\,(p.u.)$	0.257	0.319
$x_T\,(p.u.)$	0.129	0.11
$x_{ad}\,(p.u.)$	1.712	1.712
$\acute{T}_{d0}\,(p.u.)$	6.9	7.96
$H\,(s)$	4	5.1
$D\,(p.u.)$	5	3
$x_{12}\,(p.u.)$	0.55	0.55
$x_{13}\,(p.u.)$	0.53	0.53
$x_{23}\,(p.u.)$	0.6	0.6
$\omega_0\,(rad/s.)$	314.15	314.15

For RBFNNs approximators in (25), the Gaussian functions are chosen as

$$\psi_{12}(\xi_{12}) = \exp\left[\frac{-(\xi_{12}-\zeta_{1j})^T(\xi_{12}-\zeta_{1j})}{\eta_{1j}^2}\right],$$
$$\psi_{22}(\xi_{22}) = \exp\left[\frac{-(\xi_{22}-\zeta_{2j})^T(\xi_{22}-\zeta_{2j})}{\eta_{2j}^2}\right],$$

and 21 neural nodes with the centers of the basis functions ζ_{1j} and ζ_{2j} are evenly spaced in $[-63, +63] \times [-314, +314] \times [-1, +1]$ and width $\eta_{1j} = \eta_{2j} = 1$, for $j = 1, \ldots, 21$, are selected. For RBFNNs approximators in (42), the Gaussian functions are chosen as

$$\psi_{13}(\xi_{13}) = \exp\left[\frac{-(\xi_{13}-\zeta_{3j})^T(\xi_{13}-\zeta_{3j})}{\eta_{3j}^2}\right],$$
$$\psi_{23}(\xi_{23}) = \exp\left[\frac{-(\xi_{23}-\zeta_{4j})^T(\xi_{23}-\zeta_{4j})}{\eta_{4j}^2}\right],$$

17 nodes with the centers of the basis functions ζ_{3j} and ζ_{4j} are evenly spaced in $[-63, +63] \times [-314, +314] \times [-2, +2] \times [-1, +1]$ and the width $\eta_{3j} = \eta_{4j} = 1$, for $j = 1, \ldots, 17$, are selected. For RBFNNs approximators in (61), the Gaussian functions are chosen as

$$\psi_{14}(\xi_{14}) = \exp\left[\frac{-(\xi_{14}-\zeta_{5j})^T(\xi_{14}-\zeta_{5j})}{\eta_{5j}^2}\right],$$
$$\psi_{24}(\xi_{24}) = \exp\left[\frac{-(\xi_{24}-\zeta_{6j})^T(\xi_{24}-\zeta_{6j})}{\eta_{6j}^2}\right],$$

15 nodes with the centers of the basis functions ζ_{5j} and ζ_{6j} are evenly spaced in $[-63, +63] \times [-314, +3144] \times [-1, +1] \times [-1, +1] \times [-1, +1] \times [-1, +1] \times [-2, +2]$ and the width $\eta_{5j} = \eta_{6j} = 1$, for $j = 1, \ldots, 15$, are selected.

To illustrate the effectiveness of proposed control scheme for two-machine excitation system with SVC, two different cases such as keeping the desired operation points and eliminating three-phase short-circuit fault are considered. It is assumed that three-phase short-circuit fault occurs on one of the transmission lines between Generator #1 and Generator #2. The persistent external disturbance of 50% is used, i.e., $d_1 = d_2 = 0.5$ p.u..

Case 1: the operating points are

$$\begin{aligned} \delta_{10} &= 60.25^\circ,\ \omega_{10} = 314.15,\ P_{m10} = 1.08\ p.u., \\ V_{ref\,1} &= 0.95\ p.u. \\ \delta_{20} &= 60.12^\circ,\ \omega_{20} = 314.15,\ P_{m20} = 1.02\ p.u., \\ V_{ref\,2} &= 0.91\ p.u. \end{aligned}$$

To achieve the $\mathcal{L}_\infty$ norm of the tracking error, the initial values of system states and its corresponding design parameters are selected as $x_{i1}(0) = 1.2$, $y_{ri}(0) = 1.2$, $x_{i2}(0) = 0.6$, $c_{i2} = 0.6$, $x_{i3}(0) = 0.3$, $c_{i3} = 0.3$. The control objective in Case 1 is to design the control laws u_i in (49) and u_{Bi} in (65), such that the $\mathcal{L}_\infty$ tracking performance of power angles can be achieved and the power angles δ_1, δ_2, the speed ω_{10}, ω_{20}, the electrical power P_{e1}, P_{e2}, are kept in a small neighborhood of the operating points. The simulation results of Case 1 are shown in FIGUREs. 4 -10 2-8. FIGURE. 4 illustrates the power angle tracking errors of the proposed QDSC, the traditional backstepping scheme with control law *i.e.*

$$\begin{aligned} u = T_{SVC}\{&-ksin(x_1+\delta_0)e_2 \\ &-\frac{s}{\gamma^2}\Big(\frac{3\varepsilon_2 e_2^2 + c_2 + m_2 + 3\varepsilon_1 e_1^2 + \hat{\theta}}{k\sin(x_1+\delta_0)} + d_2\Big)^2 \\ &-(d_1 + d_2\hat{\theta} + 3\varepsilon_1 e_1^2 + c_1)x_2 - d_2 k\sin(x_1+\delta_0) \\ &\times (x_3 + y_{SVC0}) - \frac{s}{2\gamma^2} - d_2 a_0 + \frac{1}{T_{SVC}}(x_3 + y_{SVC0}) \\ &-\frac{1}{k\sin(x_1+\delta_0)}[m_1 x_2 + 3m_3 x_1^2 x_2 + 6\varepsilon_1 x_1 x_2^2 + \dot{\hat{\theta}} x_2 \\ &+\Big(3\varepsilon_2 e_2^2 + c_2\Big)\Big(3\varepsilon_1 e_1^2 + c_1\Big)x_2 + (3\varepsilon_2 e_2^2 + c_2 \\ &+m_2 + 3\varepsilon_1 e_1^2 + \hat{\theta})(\hat{\theta} x_2 + a_0 + k\sin(x_1+\delta_0) \\ &\times (x_3 + y_{SVC0}))] + \frac{\cos(x_1+\delta_0)x_2}{k\sin^2(x_1+\delta_0)}[m_1 x_1 + m_2 x_2 \\ &+m_3 x_1^3 + 3\varepsilon_1 x_1^2 x_2 + \hat{\theta} x_2 + a_0 + \varepsilon_2 e_2^3 + c_2 e_2] - \beta s\}, \end{aligned}$$

in [17] and [42] and PID control scheme. It is obvious that the proposed controller is much simple than traditional backstepping method and the proposed QDSC exhibits better transient performance and smaller steady tracking error, i.e. the $error_{\max} = \max(|y - y_r|)$ is applied to describe the maximum value of the tracking error, the $error_{\max}$ is 1.33×10^{-4} *p.u.* when the proposed control scheme is applied and the $error_{\max}$ is 1.98×10^{-3} *p.u.* when traditional backstepping method is used which is ten times larger than the proposed QDSC control scheme. Also, form FIGURE.4 it can be seen that the tracking error of the proposed control scheme is

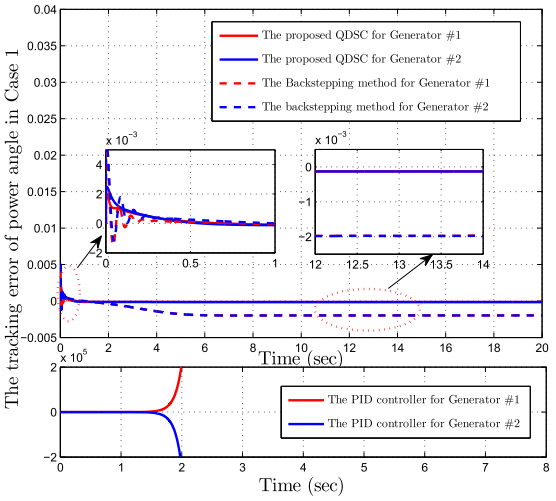

FIGURE 4. The tracking error of the power angles using the proposed QDSC, the traditional backstepping method and PID in Case 1.

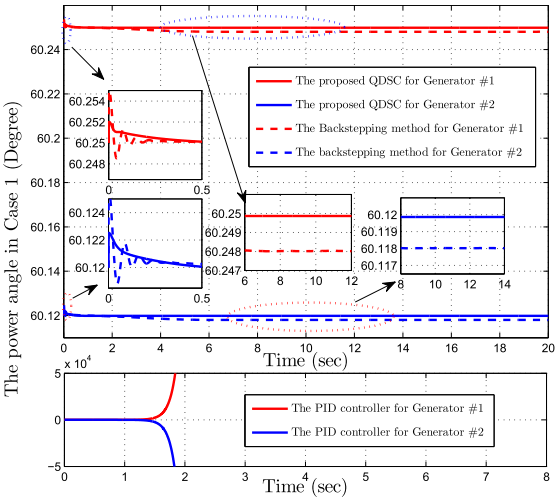

FIGURE 5. The power angles using the proposed QDSC, the traditional backstepping method and PID in Case 1.

always ($t \geq 0$) kept between -0.003 *p.u.* and $+0.003$ *p.u.* by using the initial technology in (110) − (118), which guarantees the $\mathcal{L}_\infty$ tracking performance and shows the better transient tracking performance compared with traditional backstepping method. FIGURE. 5−7 shows the curves of power angles, the rotated speed and electrical power of two generators, respectively. FIGURE. 8 illustrates the trajectory of QDSC control signal $\bar{v}_{i1}$ in (51) and the quantized control signals u_{i1} in (49). FIGURE. 9 shows the curves of accessing voltage of SVC. FIGURE. 10 illustrates the curves of $\bar{v}_{i2}$ in (67) and the quantized control input u_{Bi} in (65).

Case 2: The operating points are:

$$\begin{aligned} \delta_{10} &= 30.5^\circ,\ \omega_{10} = 314.2,\ P_{m10} = 1.06\ p.u., \\ V_{ref\,1} &= 1.20\ p.u. \\ \delta_{20} &= 30.8^\circ,\ \omega_{20} = 314.2,\ P_{m20} = 1.02\ p.u., \\ V_{ref\,2} &= 1.00\ p.u \end{aligned}$$

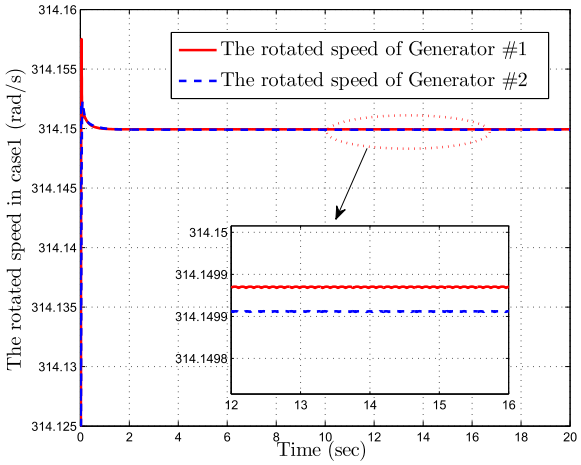

FIGURE 6. The rotated speed of the two generators in Case 1.

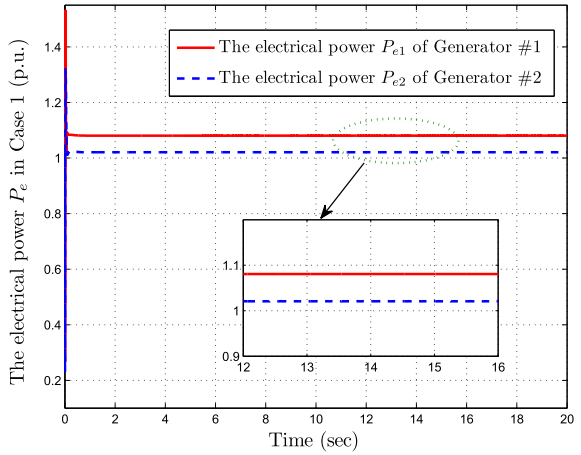

FIGURE 7. The electrical power of the two generators in Case 1.

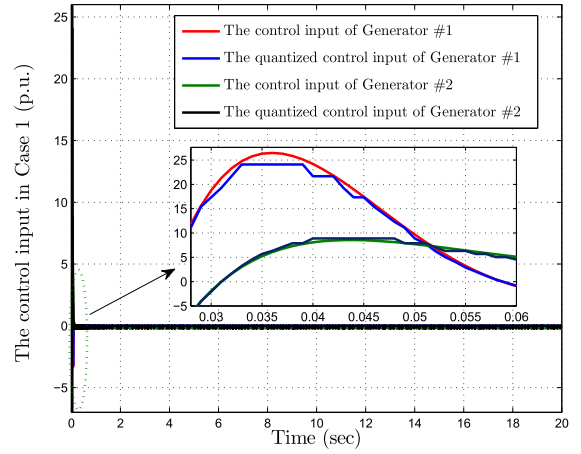

FIGURE 8. The control input of the two generators in Case 1.

We suppose that three-phase short-circuit fault occurs on the transmission line at $t = 4.8s$, and be eliminated at $t = 6.2s$. To achieve the $\mathcal{L}_\infty$ norm of tracking error, the initial values of system states and its corresponding design parameters are selected as $x_{i1}(0) = 0.8$, $y_{ri}(0) = 0.8$, $x_{i2}(0) = 0.4$,

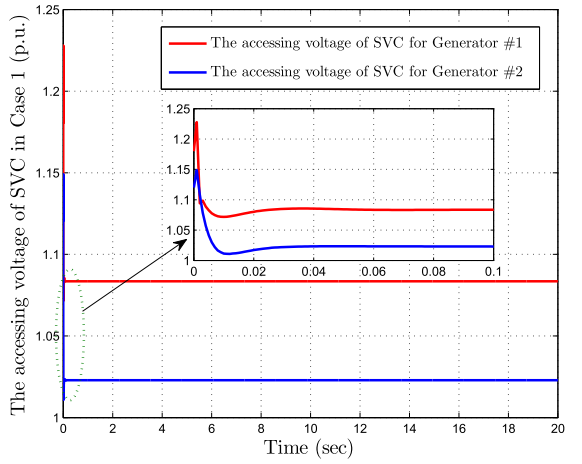

FIGURE 9. The accessing voltage of the SVC equipment for the two generators in Case 1.

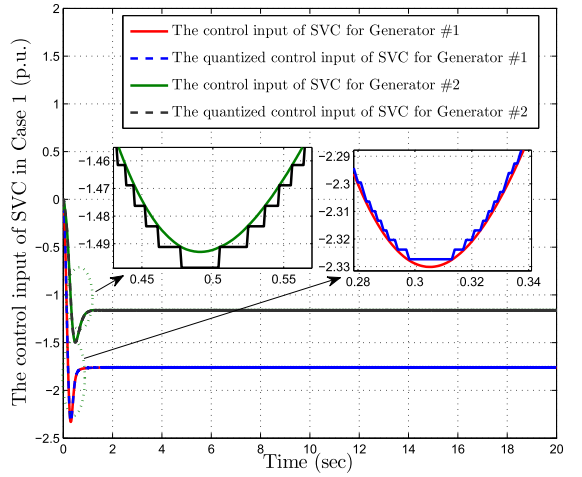

FIGURE 10. The control input of the SVC equipment in Case 1.

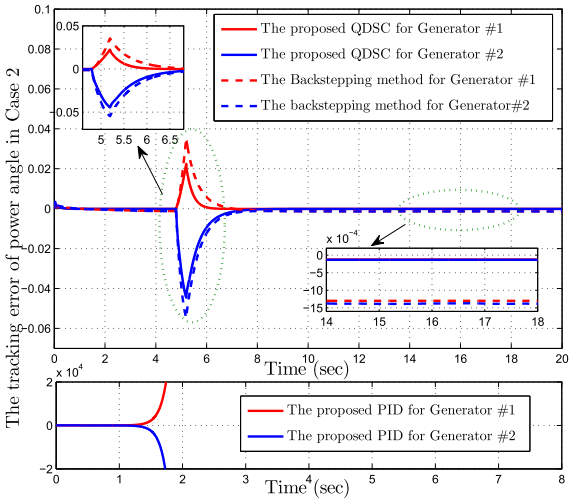

FIGURE 11. The tracking error of the power angles using the proposed QDSC and the traditional backstepping method in Case 2.

$c_{i2} = 0.4$, $x_{i3}(0) = 0.6$, $c_{i3} = 0.6$.The control objective in Case 2 is to design the control laws u_i in (49) and u_{Bi} in (65), such that the tracking performance of power angles can be

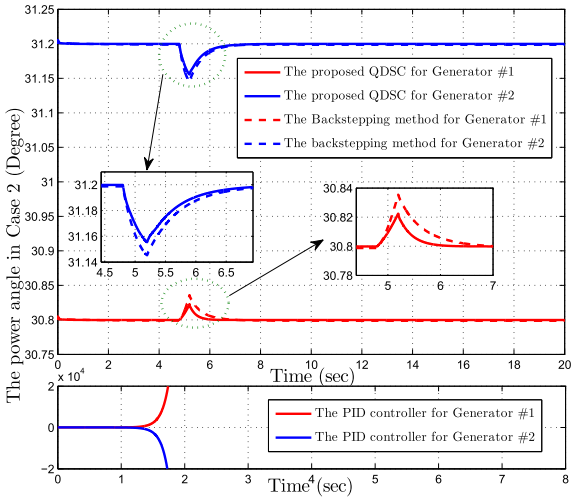

FIGURE 12. The power angles of the two generators in Case 2.

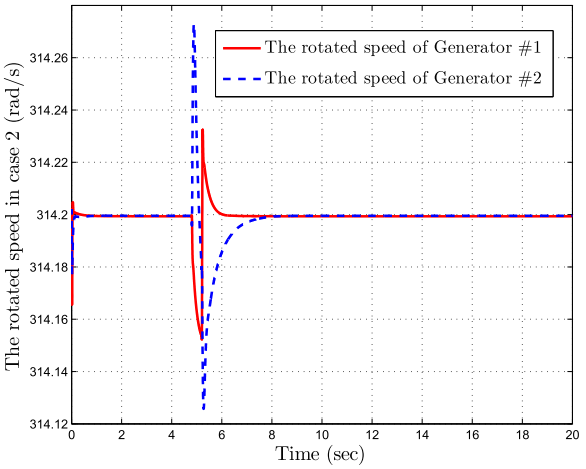

FIGURE 13. The rotated speed of the two generators in Case 2.

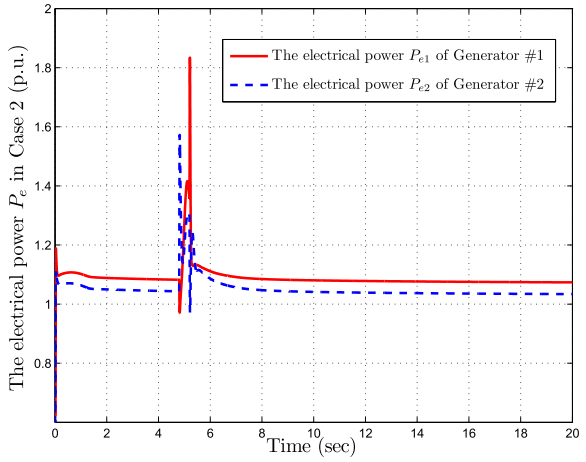

FIGURE 14. The electrical power of the two generators in Case 2.

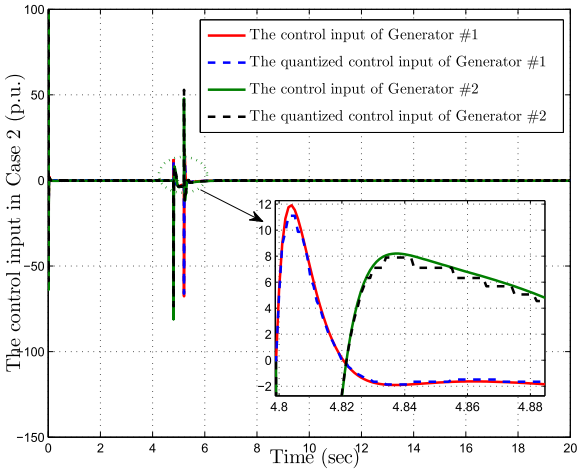

FIGURE 15. The control input of the two generators in Case 2.

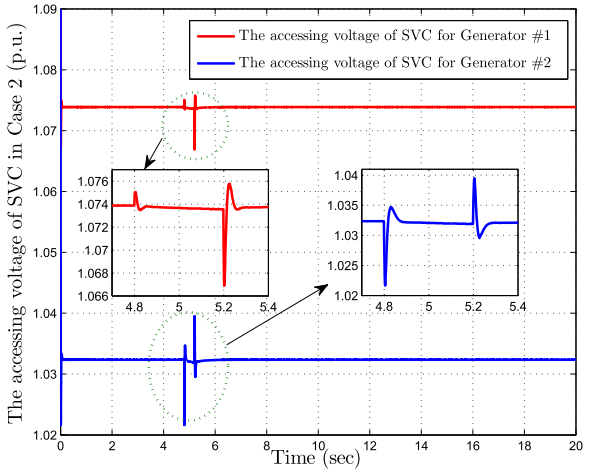

FIGURE 16. The accessing voltage of the SVC equipment for the two generators in Case 2.

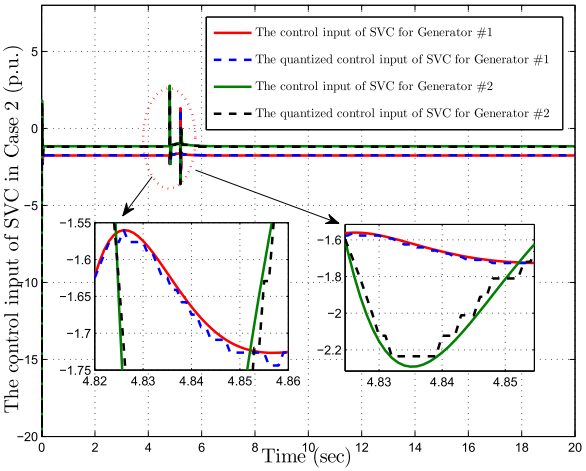

FIGURE 17. The control input of the SVC equipment in Case 2.

achieved and the power angles δ_1, δ_2, the speed ω_{10}, ω_{20} and the electrical power P_{e1}, P_{e2} are still kept in an arbitrarily small neighborhood of the operating points after the three-phase short-circuit being eliminated on the transmission line. FIGURE. (11) shows the tracking error of power angles of the two generators when three-phase short-circuit fault

occurs. Form FIGURE. (11), it can be seen that the proposed QDSC makes the power system stable rapidly (almost smaller than 1 second) and exhibits better tracking transient performance compared with traditional backstepping method after three-phase short-circuit fault is eliminated on the transmission line. FIGUREs. (12) - (17) are power angles, rotated speed, electrical powers, control input, accessing voltage of SVC and control input of the SVC of two generators when three-phase short-circuit fault occurs, respectively.

V. CONCLUSION

In this paper, a neural decentralized adaptive quantized dynamic surface control has been addressed for multi-machine excitation systems with static var compensator where the control input signal takes quantized values. The controller design is achieved by introducing a hysteretic quantizer to avoid chattering and using adaptive dynamic surface control. The advantages of the proposed method in this paper are that by combining the approximated property of the radial neural networks (RBFNNs) with the Finite Covering Lemma, the Krasovskii functionals and Razumikhin functions are removed, which leads to the achievement of $\mathcal{L}_\infty$ norm of tracking errors with the help of initializing technique. The designed controller together with the quantizer ensures semi-global stability of closed-loop system in the sense of signal boundedness. Future works will focus on the discrete-time adaptive controller design for the single or multi-machine power system. ■

APPENDIX

PROOF OF THEOREM 1

Proof: The time derivative of V in (78) yields

$$\dot{V} = \dot{V}_1 + \dot{V}_2 + \dot{V}_3 + \dot{V}_4 + \sum_{i=1}^{n} y_{i2e}\dot{y}_{i2e} + \sum_{i=1}^{n} y_{i3e}\dot{y}_{i3e}. \quad (80)$$

From (22) and (70), it arrives at

$$x_{i2} = s_{i2} + y_{i2e} + x_{2di} + c_{i2}. \quad (81)$$

By using the Young's inequalities, one has

$$s_{i1}s_{i2} \le \frac{1}{2}s_{i1}^2 + \frac{1}{2}s_{i2}^2, \quad (82)$$

$$s_{i1}y_{i2e} \le \frac{1}{2}s_{i1}^2 + \frac{1}{2}y_{i2e}^2. \quad (83)$$

Substituting (81)-(83), and the virtual control law x_{2di} in (20) into (19), we have

$$\dot{V}_1 \le \sum_{i=1}^{n}\left(-(k_{i1} - \frac{3}{2})s_{i1}^2 + \frac{1}{2}s_{i2}^2 + \frac{1}{2}y_{i2e}^2 + \frac{1}{2}c_{i2}^2\right). \quad (84)$$

Similar to (81), from (32) and (71), it arrives at

$$x_{i3} = s_{i3} + y_{i3e} + x_{3di} + c_{i3}. \quad (85)$$

By using the Young's inequalities, it follows that

$$-s_{i2}s_{i3} \le \frac{1}{2}s_{i2}^2 + \frac{1}{2}s_{i3}^2, \quad (86)$$

$$-s_{i2}y_{i3e} \le \frac{1}{2}s_{i2}^2 + \frac{1}{2}y_{i3e}^2. \quad (87)$$

Substituting (85)-(87), the virtual control law x_{3di} in (29), and adaptive law $\dot{\hat{v}}_{i2}$in (30) into (28), one has

$$\dot{V}_2 \le \sum_{i=1}^{n}(-(k_{i2} - \frac{3}{2})s_{i2}^2 + \frac{1}{2}s_{i3}^2 + \frac{1}{2}y_{i3e}^2 + \frac{1}{2}\varepsilon_{i2m}^2 + \frac{1}{2\alpha_{i2}^2} - \sigma_{i2}\tilde{v}_{i2}\hat{v}_{i2} + \frac{1}{2}c_{i3}^2). \quad (88)$$

Noting that

$$-\frac{\lambda_i s_{i3}^2\bar{v}_{i1}^2}{|s_{i3}\bar{v}_{i1}| + \varrho_{i1}} = \frac{-\lambda_i(|s_{i3}\bar{v}_{i1}|^2 - \varrho_{i1}^2) - \lambda_i\varrho_{i1}^2}{|s_{i3}\bar{v}_{i1}| + \varrho_{i1}} \le \lambda_i\varrho_{i1} - \lambda_i s_{i3}\bar{v}_{i1}, \quad (89)$$

and substituting (42)-(47) into (44), we have

$$\begin{aligned}
s_{i3}\dot{s}_{i3} &\le g_{i3}[s_{i3}(\iota_1(t)u_i + \iota_{i2}(t) + \frac{\alpha_{i3}^2 v_{i3}^* \psi_{i3}^T \psi_{i3} s_{i3}}{2}) \\
&\quad + \frac{1}{2}\varepsilon_{i3m}^2 + \frac{1}{2\alpha_{i3}^2} + \frac{1}{2}\delta_{i0}^2] \\
&\le g_{i3}[s_{i3}(-\frac{\lambda s_{i3}\bar{v}^2}{|s_{i3}\bar{v}| + \varrho_{i1}} + \iota_{i2}(t) + \frac{\alpha_{i3}^2 v_{i3}^* \psi_{i3}^T \psi_{i3} s_{i3}}{2}) \\
&\quad + \frac{1}{2}\varepsilon_{i3m}^2 + \frac{1}{2\alpha_{i3}^2} + \frac{1}{2}\delta_{i0}^2] \\
&\le g_{i3}[\lambda_i\varrho_{i1} - \lambda_i s_{i3}\bar{v}_{i1} + \frac{1}{2}s_{i3}^2 + \frac{1}{2}\varepsilon_{i3m}^2 \\
&\quad + \frac{\alpha_{i3}^2 v_{i3}^* \psi_{i3}^T \psi_{i3} s_{i3}^2}{2} + \frac{1}{2\alpha_{i3}^2} + \frac{1}{2}\delta_{i0}^2 + \frac{\bar{a}^2}{2}] \\
&\le g_{i3}[-\lambda_i s_{i3}\hat{\iota}_i\dot{\bar{v}}_{i1} + \lambda_i\varrho_{i1} + \frac{1}{2}s_{i3}^2 + \frac{\alpha_{i3}^2 v_{i3}^* \psi_{i3}^T \psi_{i3} s_{i3}^2}{2} \\
&\quad + \frac{1}{2}\varepsilon_{i3m}^2 + \frac{1}{2\alpha_{i3}^2} + \frac{1}{2}\delta_{i0}^2 + \frac{\bar{a}^2}{2}] \\
&\le g_{i3}[-s_{i3}\dot{\bar{v}}_{i1} - \lambda_i s_{i3}\tilde{\iota}_i\dot{\bar{v}}_{i1} + \lambda_i\varrho_{i1} + \frac{1}{2}\varepsilon_{i3m}^2 + \frac{1}{2}s_{i3}^2 \\
&\quad + \frac{\alpha_{i3}^2 v_{i3}^* \psi_{i3}^T \psi_{i3} s_{i3}^2}{2} + \frac{1}{2\alpha_{i3}^2} + \frac{1}{2}\delta_{i0}^2 + \frac{\bar{a}^2}{2}]. \quad (90)
\end{aligned}$$

Then, it follows that

$$\dot{V}_3 \le \sum_{i-1}^{n}(-k_{i3}s_{i3}^2 - \lambda_i s_{i3}\tilde{\iota}\dot{\bar{v}}_1 + \lambda_i\varrho_{i1} + \frac{\bar{a}^2}{2} + \frac{1}{2}\varepsilon_{i3m}^2 + \frac{1}{2\alpha_{i3}^2} + \frac{1}{2}\delta_{i0}^2 - \sigma_{i3}\tilde{v}_{i3}\hat{v}_{i3} - \lambda\sigma_\iota\tilde{\iota}\hat{\iota}). \quad (91)$$

$$\dot{V}_4 \le \sum_{i=1}^{n}(-k_{i4}s_{i4}^2 + \frac{1}{2}\varepsilon_{i4m}^2 + \frac{1}{2\alpha_{i4}^2} - \sigma_{i4}\tilde{v}_{i4}\hat{v}_{i4} + \lambda_i'\varrho_{i2} + \frac{\bar{a}^2}{2} - \lambda_i' s_{i4}\hat{\iota}_i\dot{\bar{v}}_{i2} - \lambda_i'\sigma_\iota\hat{\iota}_i\hat{\iota}_i). \quad (92)$$

From A1, the compact set

$$\Omega_r := \{(y_{ri}, \dot{y}_{ri}, \ddot{y}_{ri}) : y_{ri} + \dot{y}_{ri} + \ddot{y}_{ri} \le B_{i0}\}, \quad (93)$$

in $\Re^3$ and $B_{i0} > 0$. As shown in [28], let M_{i2} and M_{i3} to be the maximum values of B_{i2} and B_{i3} in Ω_r, respectively. Moreover, by using the Young's inequalities, the inequalities

$$|y_{i2e}B_{i2}| \leq \frac{y_{i2e}^2 B_{i2}^2}{2\mu} + \frac{\mu}{2} \leq \frac{y_{i2e}^2 M_{i2}^2}{2\mu} + \frac{\mu}{2}, \tag{94}$$

$$|y_{i3e}B_{i3}| \leq \frac{y_{i3e}^2 B_{i3}^2}{2\mu} + \frac{\mu}{2} \leq \frac{y_{i3e}^2 M_{i3}^2}{2\mu} + \frac{\mu}{2}, \tag{95}$$

$$-\sigma_{i2}\hat{\nu}_{i2}\tilde{\nu}_{i2} \leq -\frac{\sigma_{i2}}{2}\tilde{\nu}_{i2}^2 + \frac{\sigma_{i2}}{2}\nu_{i2}^{*2}, \tag{96}$$

$$-\sigma_{i3}\hat{\nu}_{i3}\tilde{\nu}_{i3} \leq -\frac{\sigma_{i3}}{2}\tilde{\nu}_{i3}^2 + \frac{\sigma_{i3}}{2}\nu_{i3}^{*2}, \tag{97}$$

$$-\sigma_{i4}\hat{\nu}_{i4}\tilde{\nu}_{i4} \leq -\frac{\sigma_{i4}}{2}\tilde{\nu}_{i4}^2 + \frac{\sigma_{i4}}{2}\nu_{i4}^{*2}, \tag{98}$$

$$-\sigma_{\iota}\tilde{\iota}_i\hat{\iota}_i \leq -\frac{\sigma_{\iota}}{2}\tilde{\iota}_i^2 + \frac{\sigma_{\iota}}{2}\iota_i^{*2}, \tag{99}$$

$$-\sigma_{\iota'}\tilde{\iota}_i'\hat{\iota}_i' \leq -\frac{\sigma_{\iota'}}{2}\tilde{\iota}_i^2 + \frac{\sigma_{\iota'}}{2}\iota_i'^{*2}, \tag{100}$$

hold with μ being a positive constant. Let

$$\frac{1}{\tau_{i2}} \geq \frac{1}{2} + \frac{M_{i2}^2}{2\mu} + \alpha_{i0}, \tag{101}$$

$$\frac{1}{\tau_{i3}} \geq \frac{\lambda}{2} + \frac{M_{i3}^2}{2\mu} + \alpha_{i0}. \tag{102}$$

Substituting (84), (88), (91), (92) and (94)-(102) into (80), it follows that

$$\begin{aligned}\dot{V} \leq \sum_{i=1}^{n}[&-(k_{i1} - \frac{3}{2})s_{i1}^2 - \left(k_{i2} - \frac{3}{2}\right)s_{i2}^2 - \left(k_{i3} - \frac{1}{2}\right)s_{i3}^2 \\ &- k_{i4}s_{i4}^2 - \alpha_{i0}y_{i2e}^2 - \alpha_{i0}y_{i3e}^2 - \frac{\sigma_{i2}}{2}\tilde{\nu}_{i2}^2 - \frac{\sigma_{i3}}{2}\tilde{\nu}_{i3}^2 \\ &- \frac{\sigma_{i4}}{2}\tilde{\nu}_{i4}^2 - \frac{\sigma\iota_i}{2}\tilde{\iota}_i^2 - \frac{\sigma\iota_i'}{2}\tilde{\iota}_i'^2] + C^*,\end{aligned} \tag{103}$$

where

$$\begin{aligned}C^* = \sum_{i=1}^{n}(&\frac{1}{2}\varepsilon_{i2m}^2 + \frac{1}{2\alpha_{i2}^2} + \frac{\sigma_{i2}}{2}\nu_{i2}^{*2} + \frac{\bar{a}^2}{2} + \frac{1}{2}\varepsilon_{i3m}^2 + \frac{1}{2\alpha_{i3}^2} \\ &+ \frac{1}{2}\delta_{i0}^2 + \frac{\sigma_{i3}}{2}\nu_{i3}^{*2} + \frac{1}{2}\varepsilon_{i4m}^2 + \frac{1}{2\alpha_{i4}^2} + \frac{\sigma_{i4}}{2}\nu_{i4}^{*2} + \frac{1}{2}c_{i2}^2 \\ &+ \lambda_i\varrho_{i1} + \mu + \frac{\sigma_{\iota}}{2}\iota_i^{*2} + \lambda_i'\varrho_{i2} + \frac{\bar{a}^2}{2} + \frac{\sigma_{\iota'}}{2}\iota_i'^{*2} + \frac{1}{2}c_{i3}^2).\end{aligned} \tag{104}$$

Here, α_{i0} is positive design parameter and satisfies

$$\begin{aligned}\alpha_{i0} \leq \min\{&g_{\min}(k_{i1} - \frac{3}{2}), g_{\min}\left(k_{i2} - \frac{3}{2}\right), g_{\min}\left(k_{i3} - \frac{1}{2}\right), \\ &k_{i4}, \frac{\gamma_{i2}\sigma_{i2}}{2}, \frac{\gamma_{i3}\sigma_{i3}}{2}, \frac{\gamma_{i4}\sigma_{i4}}{2}, \frac{\gamma_{\iota}\sigma_{\iota}}{2}, \frac{\gamma_{\iota'}\sigma_{\iota'}}{2}\}.\end{aligned} \tag{105}$$

Therefore, by using (103), it follows that

$$\dot{V} \leq -2\alpha_{i0}V + C^*. \tag{106}$$

Let

$$\alpha_{i0} > \frac{C^*}{2p}. \tag{107}$$

Then, $\dot{V} \leq 0$ on $V = p$ that implies $V \leq p$ is an invariant set, i.e., if $V(0) \leq p$, then, $V(t) \leq p$, for all $t \geq 0$. By solving the inequality (106), it follows that

$$0 \leq V(t) \leq C^*/2\alpha_{i0} + \left\{V(0) - C^*/2\alpha_{i0}\right\}e^{-2\alpha_{i0}t} \tag{108}$$

which implies

$$\lim_{t\to\infty} V(t) \leq C^*/2\alpha_{i0}. \tag{109}$$

Thus, all the signals such as $s_{i1}, s_{i2}, s_{i3}, s_{i4}, \tilde{\nu}_{i2}, \tilde{\nu}_{i3}, \tilde{\nu}_{i4}, \tilde{\iota}_i, \tilde{\iota}_i', y_{i2e}, y_{i3e}$ in the closed-loop system are ultimately uniformly bounded. It should be noted that α_{i0} can be chosen large enough by properly selecting the design parameters i.e., $k_{i1}, k_{i2}, k_{i3}, k_{i4}, \gamma_{i2}, \gamma_{i3}, \gamma_{i4}, \sigma_{i2}, \sigma_{i3}, \sigma_{i4}, \sigma_{\iota'}, \sigma_{\iota}$, leading to all the signals such as $s_{i1}, s_{i2}, s_{i3}, s_{i4}, \tilde{\nu}_{i2}, \tilde{\nu}_{i3}, \tilde{\nu}_{i4}, \tilde{\iota}, \tilde{\iota}', y_{i2e}, y_{i3e}$ in the closed-loop system can eventually converge to an arbitrary small value.

In order to achieve $\mathcal{L}_\infty$ norms of tracking errors of power angles, the initial conditions of estimations of unknown parameters in (68) and (69) are set as

$$\begin{aligned}&\hat{\nu}_{i2}(0) = 0, \quad \hat{\nu}_{i3}(0) = 0, \quad \hat{\nu}_{i4}(0) = 0, \\ &\hat{\iota}_i(0) = 0, \quad \hat{\iota}_i'(0) = 0.\end{aligned} \tag{110}$$

Also, in order to make $S_{ij}(0) = 0, j = 1, \ldots, 4$, we set

$$\begin{aligned}y_{ri}(0) &= x_{i1}(0), \\ x_{i4}(0) &= V_{refi}(0), \\ c_{i2} &= x_{i2}(0) - z_{i2}(0), \\ c_{i3} &= x_{i3}(0).\end{aligned} \tag{111}$$

Now, taking (110)-(111) into consideration, from (16), (20)-(22), (29)-(32), (49)-(54), and (70)-(71), it can ba shown in a step-by-step fashion that

$$\begin{aligned}x_{2di}(0) &= z_{i2}(0), \\ x_{3di}(0) &= 0 \Rightarrow z_{i3}(0) = 0, \\ s_{ij}(0) &= 0, \quad j = 2, 3, \\ y_{ije}(0) &= z_{ij}(0) - x_{jdi}(0) \\ &= 0, \quad j = 2, 3.\end{aligned} \tag{112}$$

Then, we have

$$V(0) = \sum_{i=1}^{n}\left(\begin{array}{c}\frac{1}{2\gamma_{i2}}\nu_{i2}^{*2} + \frac{1}{2\gamma_{i3}}\nu_{i3}^{*2} + \frac{\lambda}{2\gamma_{\iota'}}\iota_i^{*2} \\ + \frac{1}{2\gamma_{i4}}\nu_{i4}^{*2} + \frac{\lambda}{2\gamma_{\iota'}}\iota_i'^{*2}\end{array}\right). \tag{113}$$

From (104) and (105), the following inequalities hold

$$\begin{aligned}\frac{C^*}{\alpha_{i0}} = \sum_{i=1}^{n}(&\frac{1}{2\alpha_{i0}}\varepsilon_{i2m}^2 + \frac{1}{2\alpha_{i0}\alpha_{i2}^2} + \frac{\sigma_{i2}}{2\alpha_{i0}}\nu_{i2}^{*2} + \frac{\bar{a}^2}{2\alpha_{i0}} \\ &+ \frac{1}{2\alpha_{i0}}\varepsilon_{i3m}^2 + \frac{1}{2\alpha_{i0}\alpha_{i3}^2} + \frac{1}{2\alpha_{i0}}\delta_{i0}^2 + \frac{\sigma_{i3}}{2\alpha_{i0}}\nu_{i3}^{*2} \\ &+ \frac{1}{2\alpha_{i0}}\varepsilon_{i4m}^2 + \frac{1}{2\alpha_{i0}\alpha_{i4}^2} + \frac{\sigma_{i4}}{2\alpha_{i0}}\nu_{i4}^{*2} + \frac{\lambda\varrho_{i1}}{\alpha_{i0}} + \frac{\mu}{\alpha_{i0}}\end{aligned}$$

$$+\frac{\sigma_{\iota}}{2\alpha_{i0}}\iota_i^{*2}+\frac{\lambda\varrho_{i2}^{'}}{\alpha_{i0}}+\frac{\bar{a}^2}{2\alpha_{i0}}+\frac{\sigma_{\iota}^{'}}{2\alpha_{i0}}\iota_i^{*2}), \tag{114}$$

which implies

$$\begin{aligned} V(0)-\frac{C^*}{\alpha_{i0}} \leq -\sum_{i=1}^{n}\Bigg(&\frac{1}{2\alpha_{i0}}\varepsilon_{i2m}^2+\frac{1}{2\alpha_{i0}\alpha_{i2}^2}+\frac{\bar{a}^2}{2\alpha_{i0}}\\ &+\frac{1}{2\alpha_{i0}}\varepsilon_{i3m}^2+\frac{1}{2\alpha_{i0}\alpha_{i3}^2}+\frac{1}{2\alpha_{i0}}\delta_{i0}^2\\ &+\frac{1}{2\alpha_{i0}}\varepsilon_{i4m}^2+\frac{1}{2\alpha_{i0}\alpha_{i4}^2}+\frac{\lambda\varrho_{i1}}{\alpha_{i0}}\\ &+\frac{\mu}{\alpha_{i0}}+\frac{\lambda\varrho_{i2}^{'}}{\alpha_{i0}}+\frac{\bar{a}^2}{2\alpha_{i0}}\Bigg). \end{aligned} \tag{115}$$

Then, one has

$$V(0)-\frac{C^*}{\alpha_{i0}}\leq 0, \tag{116}$$

which together with (108) and (116) implies

$$0\leq V(t)\leq\frac{C^*}{\alpha_{i0}},\quad \forall t\geq 0. \tag{117}$$

Therefore, $|s_{i1}|\leq\left(\frac{C^*}{\alpha_{i0}}\right)^{\frac{1}{2}}$ and $|s_{i4}|\leq\left(\frac{C^*}{\alpha_{i0}}\right)^{\frac{1}{2}}$, for all $t\geq 0$, which means $\sup_{t\geq 0}$, $|s_{i1}|\leq\left(\frac{C^*}{\alpha_{i0}}\right)^{\frac{1}{2}}$ and $|s_{i4}|\leq\left(\frac{C^*}{\alpha_{i0}}\right)^{\frac{1}{2}}$, or in other words

$$\begin{aligned} \|s_{i1}\|_{\infty}&\leq\sqrt{\frac{C^*}{\alpha_{i0}}},\\ \|s_{i4}\|_{\infty}&\leq\sqrt{\frac{C^*}{\alpha_{i0}}} \end{aligned} \tag{118}$$

From (118), it is clear that $\mathcal{L}_{\infty}$ norm of the tracking errors s_{i1} and s_{i4} can be made arbitrarily small if a larger α_{i0} is chosen. This completes the proof of Theorem 1.

REFERENCES

[1] Y. Wang, D. J. Hill, R. H. Middleton, and L. Gao, "Transient stability enhancement and voltage regulation of power systems," *IEEE Trans. Power Syst.*, vol. 8, no. 2, pp. 620–627, May 1993.
[2] X. G. Yan, C. Edwards, S. K. Spurgeon, and J. A. M. Bleijs, "Decentralised sliding-mode control for multimachine power systems using only output information," *IEE Proc.-Control Theory Appl.*, vol. 151, no. 5, pp. 627–635, Sep. 2004.
[3] Q. Lu, S. Mei, W. Hu, F. F. Wu, Y. Ni, and T. Shen, "Nonlinear decentralized disturbance attenuation excitation control via new recursive design for multi-machine power systems," *IEEE Trans. Power Syst.*, vol. 16, no. 4, pp. 729–736, Nov. 2001.
[4] M. A. Abido, "Optimal design of power-system stabilizers using particle swarm optimization," *IEEE Trans. Energy Convers.*, vol. 17, no. 3, pp. 406–413, Sep. 2002.
[5] Y. Wang, G. Feng, D. Cheng, and Y. Liu, "Adaptive L_2 disturbance attenuation control of multi-machine power systems with SMES units," *Automatica*, vol. 42, no. 7, pp. 1121–1132, Sep. 2006.
[6] Y. Wan and J. Zhao, "Extended backstepping method for single-machine infinite-bus power systems with SMES," *IEEE Trans. Control Syst. Technol.*, vol. 21, no. 3, pp. 915–923, May 2013.
[7] J. Zhou, C. Wen, and G. Yang, "Adaptive backstepping stabilization of nonlinear uncertain systems with quantized input signal," *IEEE Trans. Autom. Control*, vol. 59, no. 2, pp. 460–464, Feb. 2014.
[8] H. Liu, Z. Hu, and Y. Song, "Lyapunov-based decentralized excitation control for global asymptotic stability and voltage regulation of multi-machine power systems," *IEEE Trans. Power Syst.*, vol. 27, no. 4, pp. 2262–2270, Nov. 2012.
[9] E. J. Davison and N. Tripathi, "The optimal decentralized control of a large power system: Load and frequency control," *IEEE Trans. Autom. Control*, vol. AC-23, no. 2, pp. 312–325, Apr. 1978.
[10] V. A. F. De Campos, J. J. Da Cruz, and L. C. Zanetta, Jr., "Robust control of electrical power systems using PSSs and bilinear matrix inequalities," *Int. J. Elect. Power Energy Syst.*, vol. 62, pp. 10–18, Nov. 2014.
[11] P. A. Ioannou, "Decentralized adaptive control of interconnected systems," *IEEE Trans. Autom. Control*, vol. AC-31, no. 4, pp. 291–298, Apr. 1986.
[12] X.-Y. Zhang, Z. Xu, and S.-L. Hu, "Decentralized adaptive neural network dynamic surface control design for multi-machine excitation systems," in *Proc. Int. Conf. IEEE Inf. Cybern. Soc. Syst.*, Aug. 2016, pp. 247–251.
[13] A. Karimi and A. Feliachi, "Decentralized adaptive backstepping control of electric power systems," *Electr. Power Syst. Res.*, vol. 78, no. 3, pp. 484–493, Jun. 2008.
[14] Z. Duan, C. Zhang, Z. Hu, and Y. Zhang, "Robust control of interconnected power system based on wams considering signals transmission delay," in *Proc. IEEE Power Energy Eng. Conf.*, Mar. 2009, pp. 1–4.
[15] X. Zhang and Y. Lin, "Adaptive control for a class of nonlinear time-delay systems preceded by unknown hysteresis," *Int. J. Syst. Sci.*, vol. 44, no. 8, pp. 1468–1482, Aug. 2013.
[16] X. Zhang, C.-Y. Su, Y. Lin, L. Ma, and J. Wang, "Adaptive neural network dynamic surface control for a class of time-delay nonlinear systems with hysteresis inputs and dynamic uncertainties," *IEEE Trans. Neural Netw. Learn. Syst.*, vol. 26, no. 11, pp. 2844–2860, Nov. 2015.
[17] X.-Y. Xu, A. Luo, L. Fang, Z.-K. Shuai, and S.-J. Peng, "New optimal nonlinear PI voltage controller for SVC," *Proc. CSEE*, vol. 29, no. 1, pp. 80–86, 2009.
[18] L. Cong, Y. Wang, and D. J. Hill, "Co-ordinated control design of generator excitation and SVC for transient stability and voltage regulation enhancement of multi-machine power systems," *Int. J. Robust Nonlinear Control*, vol. 14, nos. 9–10, pp. 789–805, Oct. 2004.
[19] G. Cao, Z. Y. Dong, Y. Wang, and P. Zhang, "VSC based series FACTS controllers for damping local mode oscillations," in *Proc. Int. Conf. IEEE Power Eng. Soc.*, Aug. 2007, pp. 1–7.
[20] T. Zabaiou, L.-A. Dessaint, F.-A. Okou, and R. Grondin, "Coordinating control of static VAR compensators and synchronous generators based on selected remote measurements," *Electr. Power Compon. Syst.*, vol. 39, no. 5, pp. 405–422, Sep. 2011.
[21] G. Nagain and L. G. Hingorani, *Understanding FACTS: Concepts and Technology of Flexible AC Transmission Systems*. New York, NY, USA: Wiley, 2000.
[22] G. Prior and M. Krstic, "Quantized-input control Lyapunov approach for permanent magnet synchronous motor drives," *IEEE Trans. Control Syst. Technol.*, vol. 21, no. 5, pp. 1784–1794, Sep. 2013.
[23] H. Richter and E. A. Misawa, "Stability analysis of discrete linear systems with quantized input and state measurements," in *Proc. IEEE Amer. Control Conf.*, vol. 3, May 2002, pp. 2392–2397.
[24] J. Guo and H. Liu, "Hammerstein system identification with quantised inputs and quantised output observations," *IET Control Theory Appl.*, vol. 11, no. 4, pp. 593–599, Aug. 2016.
[25] X. Liu, J. Zhang, and R. Huang, "Compensation for quantized input control systems with impulsive extend state observer," in *Proc. Int. Conf. IEEE Chin. Control*, Sep. 2016, pp. 7285–7290.
[26] M. Koike and Y. Chida, "Rapid vibration attenuation and height level compensation control for a pneumatic isolation table with quantized input," in *Proc. Int. Conf. IEEE Mech. Syst.*, Sep. 2012, pp. 707–712.
[27] X.-S. Xiao and L. Wu, "Decentralized adaptive tracking of interconnected non-affine systems with time delays and quantized inputs," *Neurocomputing*, vol. 141, pp. 194–201, Oct. 2014.
[28] C. Wang and Y. Lin, "Adaptive dynamic surface control for linear multivariable systems," *Automatica*, vol. 46, no. 10, pp. 1703–1711, Oct. 2010.
[29] D. Swaroop, J. K. Hedrick, P. P. Yip, and J. C. Gerdes, "Dynamic surface control for a class of nonlinear systems," *IEEE Trans. Autom. Control*, vol. 45, no. 10, pp. 1893–1899, Oct. 2000.
[30] Y. Guo, D. J. Hill, and Y. Wang, "Nonlinear decentralized control of large-scale power systems," *Automatica*, vol. 36, no. 9, pp. 1275–1289, 2000.
[31] X.-Y. Zhang, C.-P. Liu, J.-G. Wang, and L. Yan, "Adaptive dynamic surface control for generator excitation control system," *Math. Problems Eng.*, vol. 2014, no. 7, pp. 1–11, 2014.

[32] M. Chen and J. Yu, "Adaptive dynamic surface control of NSVs with input saturation using a disturbance observer," *Chin. J. Aeronaut.*, vol. 28, no. 3, pp. 853–864, 2015.
[33] C. Wang, C. Wen, Y. Lin, and W. Wang, "Decentralized adaptive tracking control for a class of interconnected nonlinear systems with input quantization," *Automatica*, vol. 81, pp. 359–368, Jul. 2017.
[34] T. Hayakawa, H. Ishii, and K. Tsumura, "Adaptive quantized control for nonlinear uncertain systems," *Syst. Control Lett.*, vol. 58, no. 9, pp. 625–632, 2009.
[35] X. Zhang, Y. Wang, C. Wang, C.-Y. Su, Z. Li, and X. Chen, "Adaptive estimated inverse output-feedback quantized control for piezoelectric positioning stage," *IEEE Trans. Cybern.*, to be published, doi: 10.1109/TCYB.2018.2826519.
[36] X. Zhang *et al.*, "Decentralized adaptive neural approximated inverse control for a class of large-scale nonlinear hysteretic systems with time delays," *IEEE Trans. Syst., Man, Cybern. Syst.*, to be published, doi: 10.1109/TSMC.2018.2827101.
[37] X. Xia and T. Zhang, "Adaptive output feedback dynamic surface control of nonlinear systems with unmodeled dynamics and unknown high-frequency gain sign," *Neurocomputing*, vol. 143, pp. 312–321, Nov. 2014.
[38] Y. Li, S. Tong, L. Liu, and F. Gang, "Adaptive output-feedback control design with prescribed performance for switched nonlinear systems," *Automatica*, vol. 80, pp. 225–231, Jun. 2017.
[39] B. Ren, S. S. Ge, C.-Y. Su, and T. H. Lee, "Adaptive neural control for a class of uncertain nonlinear systems in pure-feedback form with hysteresis input," *IEEE Trans. Syst., Man, Cybern. B, Cybern.*, vol. 39, no. 2, pp. 431–443, Apr. 2009.
[40] R. M. Sanner and J.-J. E. Slotine, "Gaussian networks for direct adaptive control," *IEEE Trans. Neural Netw.*, vol. 3, no. 6, pp. 837–863, Nov. 1992.
[41] D. Wang and J. Huang, "Neural network-based adaptive dynamic surface control for a class of uncertain nonlinear systems in strict-feedback form," *IEEE Trans. Neural Netw.*, vol. 16, no. 1, pp. 195–202, Jan. 2005.
[42] L. Sun, S. Tong, and Y. Liu, "Adaptive backstepping sliding mode H_∞ control of static VAR compensator," *IEEE Trans. Control Syst. Technol.*, vol. 19, no. 5, pp. 1178–1185, Sep. 2011.
[43] S. Song, J. Liu, and H. Wang, "Adaptive neural network control for uncertain switched nonlinear systems with time delays," *IEEE Access*, vol. 6, pp. 22899–22907, 2018.
[44] J. Cai, J. Wan, H. Que, Q. Zhou, and L. Shen, "Adaptive actuator failure compensation control of second-order nonlinear systems with unknown time delay," *IEEE Access*, vol. 6, pp. 15170–15177, 2018.
[45] S. S. Ge and C. Wang, "Adaptive neural control of uncertain MIMO nonlinear systems," *IEEE Trans. Neural Netw.*, vol. 15, no. 3, pp. 674–692, May 2004.

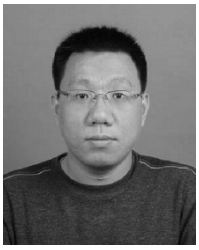

XIUYU ZHANG (M'17) was born in Jilin, China. He received the B.S. and M.S. degrees from Northeast Electric Power University, Jilin, in 2003 and 2006, respectively, and the Ph.D. degree from the Beijing University of Aeronautics and Astronautics, Beijing, China, in 2012.

He is currently a Professor with the School of Automation Engineering, Northeast Electric Power University. His research interests include robust and adaptive control for nonlinear systems with smart material-based actuators.

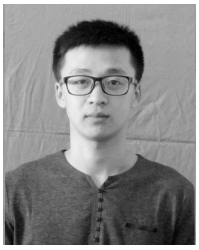

BIN LI was born in Heze, China. He received the B.S. degree from the Shandong University of Technology, Zibo, China, in 2016. He is currently pursuing the master's degree with Northeast Electric Power University, Jilin, China.

His research interests include robust and adaptive control for nonlinear systems with smart material-based actuators.

GUOQIANG ZHU was born in Heze, China. He received the B.S. and M.S. degrees from Northeast Electric Power University, Jilin, China, in 2003 and 2007, respectively, and the Ph.D. degree from the Beijing University of Aeronautics and Astronautics, Beijing, China, in 2015.

He is currently an Associate Professor with the School of Automation Engineering, Northeast Electric Power University. His research interests include robust and adaptive control for nonlinear systems.

XINKAI CHEN (SM'02) received the Ph.D. degree in engineering from Nagoya University, Japan, in 1999. He is currently a Professor with the Department of Electronic and Information Systems, Shibaura Institute of Technology, Japan. His research interests include adaptive control, smart materials, hysteresis, sliding mode control, machine vision, and observer. He has also severed for international conferences as organizing committee members, including program chairs and program co-chairs. He has served as an Associate Editor for several journals, including the IEEE TRANSACTIONS ON AUTOMATIC CONTROL, the IEEE TRANSACTIONS ON CONTROL SYSTEMS TECHNOLOGY, the IEEE/ASME TRANSACTIONS ON MECHATRONICS, and the *European Journal of Control*.

MIAOLEI ZHOU (M'14) was born in 1976. He received the B.S. and M.S. degrees in industrial electric automation from the Jilin Institute of Technology, China, in 1997 and 2000, respectively, and the Ph.D. degree in control theory and control engineering from Jilin University in 2004. From 2006 to 2008, he was a Post-Doctoral Researcher with Tokyo University, Japan.

In 2000, he joined the Department of Control Science and Engineering, Jilin University, where he became an Associate Professor in 2009 and a Professor in 2014. He has supervised over 20 research projects, including the National Natural Science Funds of China and the National High Technology Research and Development Program. He has authored over 70 papers. His research interests include micro-/nano-drive and control technology, nonlinear control theory, and navigation and control of robot. He is an Editorial Board Member of the Scientific Journal of Control Engineering.